Role of Interferon-γ in the inflammatory response following disc herniation

A study of nociception and genetic susceptibility in acute lumbar radicular pain

Gunn-Helen Moen

Master Thesis

The Department of Biosciences, Faculty of Mathematics and Natural Sciences, University of Oslo, Norway

National Institute of Occupational Health, Oslo, Norway

May 2014

Role of Interferon-γ in the inflammatory response following disc herniation

A study of nociception and genetic susceptibility in acute lumbar radicular pain

2014

Role of Interferon-γ in the inflammatory response following disc herniation

Author: Gunn-Helen Moen

http://www.duo.uio.no/

Press: Reprosentralen, University of Oslo

Acknowledgments

All the laboratory work in this thesis was carried out at the National Institute of Occupational Health (STAMI), Oslo, Norway.

Firstly, I would like to thank my supervisor Johannes Gjerstad for the opportunity to work with such a fascinating subject. Thank you for always being available to answer questions, for your enthusiasm regarding my project, for pushing me to reach my potential and for always sharing your knowledge.

I am also grateful for all the encouragement from Aurora Moen, my co-supervisor. Thank you for always having an open door, for all your patience in the animal lab, for help with statistics and for comments on my writing, but mostly for always having something positive to say.

Furthermore, I thank Ada Ingvaldsen for all the laboratory training, for excellent DNA isolation, and for always having time to answer any questions. I also thank the staff at the animal facility for taking care of the animals.

In addition I would like to thank all my co-workers at STAMI. Thanks for always keeping a positive atmosphere at work, for pleasant lunches and exciting conversations.

To my fellow students at UiO and STAMI, thank you for always being good company, for the coffee breaks and inspiring discussions.

In the end, I would like to thank my family and friends. Thanks for always supporting me, for making me laugh and for always having time to listen. A special thanks to Kim for help with the writing of the thesis, for your kind words and for all your love and support.

Gunn-Helen Moen

Oslo, May 2014

Abstract

Lumbar radicular pain after intervertebral disc herniation may be associated with mechanical compression of the nerve roots, but also release of pro-inflammatory cytokines from nucleus pulposus (NP) tissue. In an animal model mimicking the clinical situation after disc herniation, we examined the pro-inflammatory and pro-nociceptive effect of NP tissue exposed to the dorsal nerve roots.

Using quantitative polymerase chain reaction (qPCR), an up-regulation of interferon (IFN)-γ, IFN-α2, IFN-1β and IFN-α4 in NP tissue exposed to the spinal dorsal nerve roots for one hour was demonstrated. Moreover, the data indicated a significant up-regulation of cluster of differentiation 68 (CD68), corresponding to an increase in lysosomal activity and macrophage activation. A correlation between IFN-γ, known to activate macrophages, and CD68 was also observed. However, F4/80, a marker specific for blood-borne macrophages, was not detected. This suggests that tissue-specific macrophages within NP are activated after disc herniation.

As in previous studies, single cell recordings of the dorsal horn neurons showed significant increase in the C-fibre response when NP was applied onto the spinal dorsal nerve roots. Moreover, IFN-γ had a similar effect as NP tissue, with a clear increase in C-fibre response, suggesting that IFN-γ released from the herniated disc may have an important pro-nociceptive and pro-inflammatory effect.

To follow up the findings from the animal study three IFN-γ single nucleotide polymorphisms (SNPs) (rs2069705, rs1861494 and rs2069718) were studied in patients with acute lumbar radicular pain due to disc herniation. The data showed a clear trend regarding pain intensity measured with visual analogue scale (VAS), and significant differences regarding function and disability, measured with oswestry disability index (ODI). This suggests that the SNPs may be involved in determining the transcription rate of IFN-γ.

In summary, our data show that tissue-specific, not circulating, macrophages are important in the patophysiological response following disc herniation. Further, the results indicate that IFN-γ may be important for the increased excitability of dorsal horn neurons induced by NP. The present study suggests that IFN-γ has an important role in acute lumbar radicular pain due to disc herniation.

Table of contents

Abbreviations

A	Adenosine
AF	Annulus fibrosus
AMPA	α-Amino-3-hydroxy-5-methyl-4-isoxazolepropionic acid
ANOVA	Analysis of variance
ASIC3	Acid sensing ion channel 3
ATP	Adenosine-tri-phosphate
BDNF	Brain-derived neurotrophic factor
Bp	Base pair
C	Cytosine
CAMKII	Ca^{2+}-calmodulin dependent kinase II
CD68	Cluster of differentiation 68
CD68+	Cluster of differentiation 68 positive cells
cDNA	Complimentary deoxyribonucleic acid
CEBPB	CCAAT/Enhancer binding protein-β
CNS	Central nervous system
CSF	Colony-stimulating factor
C_t-value	Cycle threshold-value
DNA	Deoxyribonucleic acid
DRG	Dorsal root ganglion
ERK	Extracellular signal related kinase
G	Guanine
Glu	Glutamate
GluR1	Glutamate receptor 1
GP	General Practitioner
HUS	Haukeland university hospital

IASP	International Association for the Study of Pain
IFN	Interferon
IL	Interleukin
iNOS	inducible nitric oxide synthase
IP_3	Inositol-1,4,5-triphosphate
JAK	Janus kinase
mGlu	metabotropic glutamate receptor
MRI	Magnetic resonance imaging
mRNA	messenger ribonucleic acid
NGF	Nerve growth factor
NK1	Neurokinin-1 receptor
NMDA	N-methyl-D-aspartate
NO	Nitric oxide
NP	Nucleus pulposus
NS	Nociceptive specific
NTC	Non-template control
ODI	Oswestry disability index
OUS	Oslo university hospital
PAG	Periaqueductal gray
PCR	Polymerase chain reaction
PKA	Protein kinase A
PLC	Phospholipase C
qPCR	Quantitative polymerase chain reaction
RIN	RNA integrity number
RNA	Ribonucleic acid
RNase	Ribonuclease
SEM	Standard error of the mean

SLE	Systemic lupus erythematosus
SNP	Single nucleotide polymorphisms
SP	Substance P
STAT	Signal transducer and activator of transcription
T	Tyrosine
TE-buffer	tri-ethylenediaminetetraacetic acid-buffer
TGF	Transforming growth factor
T_m	Melting temperature
TNF	Tumor necrosis factors
TRPV1	Transient receptor potential cation channel subfamily V member 1
U	Units
VAS	Visual analogue scale
WDR	Wide dynamic range

1 Introduction

"The girl who feels no pain was in the kitchen, stirring ramen noodles, when the spoon slipped from her hand and dropped into the pot of boiling water. … Without thinking, Ashlyn Blocker reached her right hand in to retrieve the spoon, then took her hand out of the water and stood looking at it under the oven light. She walked a few steps to the sink and ran cold water over all her faded white scars."

The Hazards of Growing Up Painlessly, NY Times 15.11.12

Pain is an essential warning device that alerts us to the presence of damaging stimuli, and all living organisms need to be able to react to noxious stimuli (Woolf and Salter 2000). People like Ashlyn Blocker, who suffers from congenital insensitivity to pain, are in constant danger of hurting themselves without knowing.

1.1.1 Pain vs. nociception

According to the International Association for the Study of Pain (IASP), pain is defined as an unpleasant sensory and emotional experience associated with actual or potential tissue damage or described in terms of such damage. According to this definition pain is an experience and no tissue damage is needed to feel pain. The pain experience is not only the result of sensory signaling, but also attention, understanding, control, expectations and emotion (McGrath 1994). In contrast, nociception is defined by IASP as the neural process of encoding noxious stimuli, and is the sensory component of pain. For review see (Tracey 2008).

Pain can be subdivided into three categories: nociceptive pain, inflammatory pain and pathological pain. Nociceptive pain gives information about dangerous stimuli in the environment. This form of pain is clearly adaptive, because it helps us to avoid tissue damage. Inflammatory pain is also a type of adaptive pain, leading to protection of injured tissue and healing. The last category is pathological pain, which is not adaptive, but a disease of the nervous system. For review see (Woolf 2010).

1.2 Inflammatory pain

Inflammation is part of the non-specific immune response to noxious stimuli, such as infection or injury. During an inflammation, white blood cells are recruited to the injured area. In the acute phase tissue-resident macrophages, as well as mast cells, increase their production of inflammatory mediators, such as cytokines, which mediate the inflammatory responses at the site of injury. For review see (Medzhitov 2008).

Nociceptors are specialized high threshold sensory receptors. They respond to a variety of noxious stimuli, including chemical, mechanical or thermal stimuli, which have the potential to cause tissue damage. Nociceptor activation is modulated by local chemicals that are released upon tissue damage, such as bradykinin, serotonin, adenosine-tri-phosphate (ATP), protons and nerve growth factor (NGF). The nerve cells can also release neurotransmitters, like substance P (SP), which can facilitate production of inflammatory mediators by adjacent immune cells. These chemicals can sensitize the peripheral nociceptors by lowering their activation threshold to both thermal and mechanical stimuli (Rang *et al.* 1991), leading to primary hyperalgesia. This increased pain sensitivity at an injury site is categorized as inflammatory pain. For review see (Julius and Basbaum 2001).

A successful inflammatory response transits from the acute phase to a repair phase, which is mainly mediated by tissue-resident and recruited macrophages. Here, the macrophages switch from producing pro-inflammatory mediator to anti-inflammatory mediators (Serhan and Savill 2005).

1.2.1 Cytokines

Cytokines are small proteins with a molecular mass of about 250 kDa. They are primarily synthesized and released by immune cells, such as T-cells and macrophages in the periphery and glia cells in the central nervous system (CNS). However, many other cell types can be able to synthesize cytokines in response to an external stimulus.

There are several major classes of cytokines; interleukins (ILs), tumor necrosis factors (TNFs), interferons (IFNs), colony-stimulating factors (CSFs), transforming growth factors (TGFs) and chemokines. For review see (Rothwell *et al.* 1996).

Cytokines can be pro- or anti-inflammatory, meaning that they can facilitate or inhibit inflammation. Pro-inflammatory cytokines such as IL-1, TNF-α and IFN-γ are able to induce their own synthesis, as well as play an important role in mediating the acute inflammatory reaction. They can for instance start cascades that increase production of other mediators such as chemokines, inducible nitric oxide synthase (iNOS), prostaglandins, cyclooxygenase-2 and other cytokines. All pro-inflammatory cytokines can have a localized effect on injured tissue, or promote a systemic manifestation. Anti-inflammatory cytokines are on the other hand able to suppress the synthesis of pro-inflammatory cytokines as well as their own, and can thereby control the inflammatory response. The major anti-inflammatory cytokines include IL-4, IL-10, IL-13 and TNF-β. For review see (Dinarello 2000)

IFN-γ

IFN-γ is an important mediator of immunity and inflammation. The cytokine is produced by activated T-cells as well as macrophages, myeloid cells, dendritic cells and natural killer cells.

IFN-γ utilizes the Janus kinase (JAK) by binding to the IFN-γ receptor (associated with JAK 1 and 2), which in turn activates signal transducer and activator of transcription (STAT). The receptor can be found at the surface of almost all cells, and the many functions of IFN-γ include STAT1-mediated induction of immune effector genes and IFN-γ mediated cross-regulation of cellular responses to other cytokines and inflammatory factors. IFN-γ is also a key component in the activation of macrophages. For review see (Hu and Ivashkiv 2009).

In addition to activating macrophages it is also suggested that IFN-γ can activate microglia (Tsuda *et al.* 2009) and astrocytes (Hashioka *et al.* 2011) in the CNS. IFN-γ may also have a neurotoxic effect.

1.3 The intervertebral disc

The spinal cord is divided into four regions (cervical, thoracic, lumbar and sacral), corresponding to the adjacent vertebrae. The human spine have 7 cervical, 12 thoracic, 5 lumbar and 5 sacral vertebrae in contrast to a rat which has 7 cervical, 13 thoracic, 6 lumbar and 4 sacral in addition to 27-30 caudal tail vertebrae.

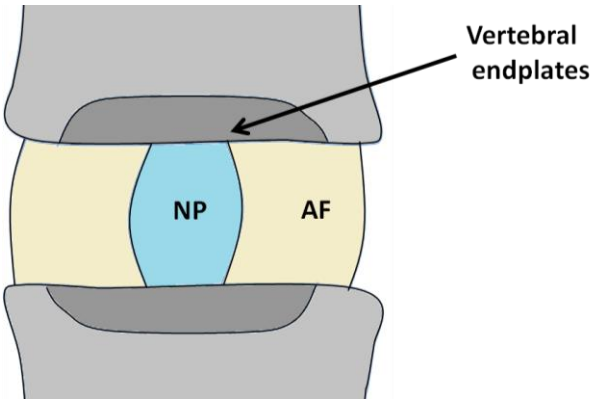

Figure 1.1: Anatomy of the intervertebral disc. A schematic overview of the intervertebral disc, with the vertebral endplates, AF and NP. The intervertebral disc separates the vertebrae, and is a shock absorber during activity. AF: Annulus Fibrosus; NP: Nucleus Pulposus.

The intervertebral disc separates the vertebrae. It functions as a shock absorber during activity and protects nerves that run down the spinal cord. The intervertebral disc is composed of four tissue components, and a schematic overview is illustrated in figure 1.1. The outer annulus fibrosus (AF) is a ring of densely packed collagen fibril lamella. The second layer is a fibrocartilaginous inner AF. The tissue consist of 10-20 lamella of collagen fibrils, mostly type I and II, which make up about 70 % of the dry weight (Eyre and Muir 1977). This provides strength to the disc. A thin transition zone separates the AF from the inner gelatinous nucleus pulposus (NP) tissue. The structure consists mainly of proteoglycans, which make up 65 % of the dry weight. Water is held together by a network of collagen type II and elastic fibres. Osmotic pressure drives water into the disc (Johnstone and Bayliss 1995). Vertebral endplates, consisting of hyaline cartilage, calcified cartilage and bone, form the superior and inferior boundaries of the disc. NP is not a vascularized structure, and nutrients are supplied from the endplate via diffusion. For review see (Urban and Roberts 2003).

1.3.1 Nucleus pulposus

NP tissue consists of small chondrocyte-like cells, present at a low density. These cells can be divided into phagocytic cells and non-phagocytic cells. The phagocytic NP cells are distinguished from the others by their large amount of endoplasmic reticulum and lysosomes. The presence of primary and secondary lysosomes reflects the phagocytic activity (Chen *et al.* 2013). Phagocytic NP cells have both morphologic trademarks of NP cells and macrophages. They might therefore be classified as tissue-specific macrophages (Nerlich *et al.* 2002).

Cluster of differentiation 68 (CD68) proteins are found in the lysosomal membrane (Holness and Simmons 1993), and are thought to protect the membrane from the hydrolytic enzymes within the lysosome (Holness *et al.* 1993). About 10-15 % of the CD68 proteins can be found on the cell membrane, and CD68 can therefore be used as a membrane marker for CD68 positive (CD68+) macrophages. The amount of lysosomes increase with activation of macrophages (Cohn *et al.* 1966). An increase in CD68 expression can therefore represent activation of macrophages, such as tissue-specific NP macrophages. However, CD68 is not specific for cells from the myeloid lineage (Gottfried *et al.* 2008), and cannot be used to investigate macrophage infiltration.

F4/80 is a transmembrane receptor located on the cell membrane, and a homolog to human epidermal growth factor module-containing mucin-like receptor 1 (EMR1). The expression of F4/80 does not represent lysosomal activity and macrophage activation, like CD86. However, studies have shown it to be the best marker for macrophages from the myeloid lineage, and F4/80 expression in tissue can therefore be an indicator of macrophage infiltration (Khazen *et al.* 2005).

1.3.2 Disc herniation

The intervertebral disc gradually degenerates when aging. The proteoglycan content in NP decreases, which is followed by a drop in osmotic pressure and loss of hydration. In addition, the relative amount of collagen types in AF will change and the fibronectin content will increase. All these changes lead to a less hydrostatic disc and a weaker and stiffer AF. Degeneration is sometimes followed by tears in the AF, which in some situations causes rupture and leakage of NP into the spinal canal, resulting in disc herniation. The rupture and

subsequent disc herniation is associated with mechanical compression of the nerve roots. For review see (Buckwalter 1995).

Other than aging, degeneration of the intervertebral disc is most likely mediated by the abnormal production of pro-inflammatory molecules secreted by NP cells, AF cells and macrophages (Rand *et al.* 1997). Pro-inflammatory mediators associated with intervertebral disc degeneration include TNF-α, IL-1β, IL-6 and IFN-γ (Le Maitre *et al.* 2005; Seguin *et al.* 2005; Shamji *et al.* 2010; Cuellar *et al.* 2013). These proteins can lead to nerve ingrowths and extracellular matrix degradation, thus facilitating the formation of tears and clefts in the intervertebral disc tissues, possibly leading to herniation.

As described above NP is not a vascularized structure and may be recognized as non-self when in contact with immune cells. Disc degeneration can therefore promote immune cell activation and immune cell migration. Infiltration of macrophages, neutrophils, T-cells and invading blood vessels has been shown in herniated discs (Kokubo *et al.* 2008; Shamji *et al.* 2010). The migration of immune cells into the intervertebral disc is also accompanied by the appearance of nociceptive nerve fibres from the dorsal root ganglion (DRG) (Freemont *et al.* 2002). NP and the potential infiltrating immune cells continue to release cytokines as well as neurotrophins (such as NGF and brain-derived neurotrophic factor (BDNF)), enhancing the inflammatory process.

In the DRG, neurotrophins (like NGF and BDNF) induces expression of neuronal pain-associated cation channels (in particular acid sensing ion channel 3 (ASIC3) and transient receptor potential cation channel subfamily V member 1 (TRPV1)) (Mamet *et al.* 2003; Zhang *et al.* 2005; Ohtori *et al.* 2006). These ion channels may promote discogenic pain and reinforce cytokine-mediated intervertebral disc degeneration. This pathogenic cascade may explain the relationship between intervertebral disc degeneration and low back pain.

The relationship between some of the factors that can contribute to disc herniation and lumbar radicular pain is illustrated in figure 1.2.

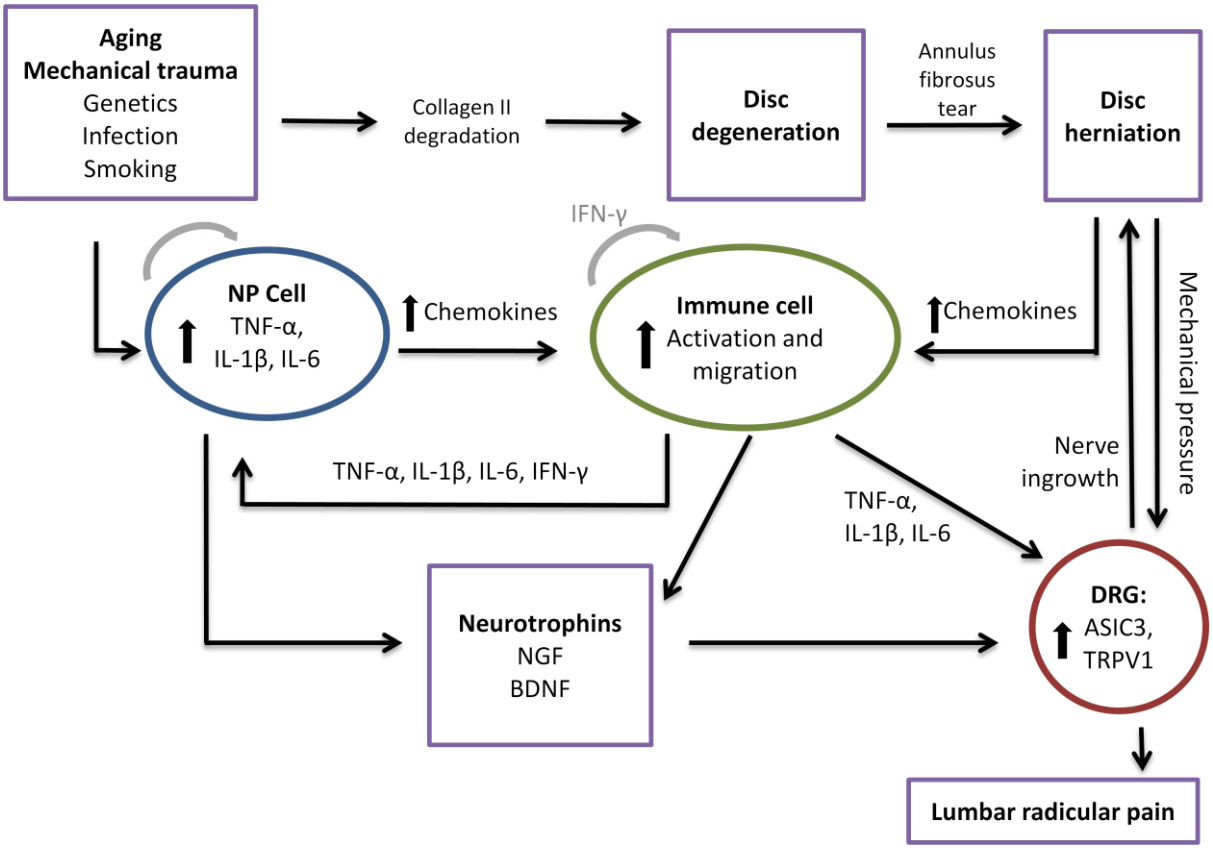

Figure 1.2: Overview of factors leading to disc herniation and lumbar radicular pain. Factors such as aging, mechanical trauma and genetics can cause degeneration of collagen and/or an abnormal production of pro-inflammatory cytokines. Degeneration of collagen type II will be followed by a drop in osmotic pressure and loss of hydration. This will lead to a less hydrostatic disc and a weaker and stiffer AF. These changes can sometimes lead to a rupture and disc herniation. Abnormal production of pro-inflammatory cytokines by NP can lead to an increase in chemokines concentration and the activation of immune cells. An increase in production of chemokines will also follow after a disc herniation. Activation of immune cells can lead to an increased production, and release, of many cytokines (including IFN-γ, IL-1β, IL-6 and TNF-α) effecting both NP and DRG. NP cells and immune cells can also produce neurotrophins (such as NGF and BDNF), which can influence the DRG to increase the expression of neuronal pain-associated cation channels (such as ASIC3 and TPRV1). The increase expression pro-inflammatory cytokines and neurotrophins can also lead to nerve ingrowth. All these factors may in the end contribute to lumbar radicular pain. AF: Annulus Fibrosus; ASIC3: Acid Sensing Ion Channel 3; BDNF: Brain-Derived Neurotrophic Factor; DRG: Dorsal Root Ganglion; IFN-γ: Interferon-γ; IL-1β: Interleukin-1β; IL-6: Interleukin-6; NGF: Nerve Growth Factor; NP: Nucleus Pulposus; TNF-α: Tumor Necrosis Factor-α; TRPV1: Transient Receptor Potential cation channel subfamily V member 1. Adapted from (Risbud and Shapiro 2014).

1.4 Pain signaling

In most cases, the pain experience starts with the activation of high threshold nociceptors located on nerve endings. The signals from the nociceptors are carried to the CNS by the aid of two types of primary sensory fibres: Aδ-fibres and C-fibres. Aδ-fibres are small, unmyelinated fibres and transmit cold, fast pain and mechanical stimuli at a speed of 12-30 m/sec. The C-fibres are larger, unmyelinated fibres and have a slower transduction speed of 0.5-2 m/sec. They transmit a duller, more diffuse slow pain. The primary afferent fibres conduct the sensory information via the DRG to the spinal dorsal horn where neurotransmitters are released in the synapse between the primary afferent fibres and the secondary afferent fibres in the dorsal horn. The incoming information is processed by the complex circuit system. For review see (Basbaum *et al.* 2009).

1.4.1 The spinal cord

The spinal cord is protected by three layers of membrane, called the meninges. These membranes lie between the bone and the tissue of the CNS. Dura mater is the thickest of the three and lies closest to the bone. The arachnoid membrane is in the middle and closest to the spinal cord is the thin pia mater. The CNS is also protected with intestinal fluid on the inside of pia mater and cerebrospinal fluid between the pia mater and the arachnoid membrane.

Each of the spinal regions (cervical, thoracic, lumbar and sacral) is subdivided into segments, giving rise to a bilateral pair of spinal nerves. The spinal nerve splits into two just before entering the spinal cord and the two branches are called roots. Incoming sensory information is carried by the dorsal root and the afferent fibres synapse with post-synaptic cells within the gray matter of the dorsal horn. An anatomic overview is illustrated in figure 1.3A.

(A) **(B)**

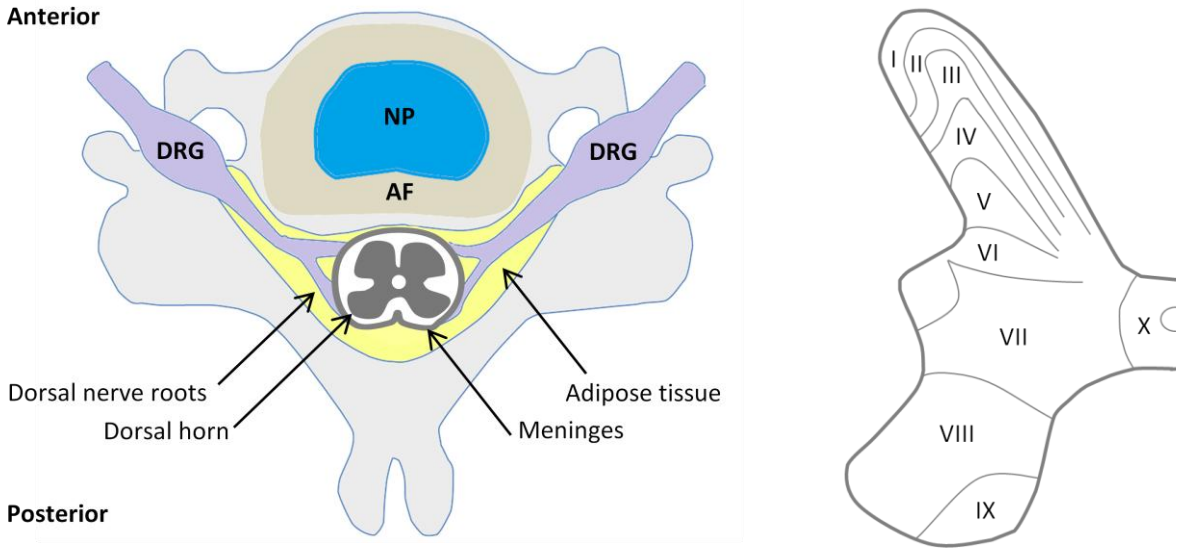

Figure 1.3: Anatomy of the spinal cord. A) Cross section of the spinal cord with adjacent structures. B) Cross section of the left side of the spinal cord gray matter (laminae I-X), with the dorsal horn on top and the ventral horn at the bottom. AF: Annulus Fibrosus; DRG: Dorsal Root Ganglion; NP: Nucleus Pulposus.

The gray matter of the spinal cord can be divided into ten laminae, according to cellular structure, called Rexed laminae (Rexed 1952) (figure 1.3B). The system labels the position of the gray columns in the spinal cord and can be divided into three groups; the anterior grey column (known as the ventral horn), the posterior grey column (known as the dorsal horn), and the lateral grey column (a part of the sympathetic nervous system that receives input from the brain stem, hypothalamus and organs). Laminae I-VI constitutes the dorsal horn and lamina VIII-IX is the ventral horn. Laminae I and II obtain information from afferent neurons that sense pain, temperature and itching. Laminae III and IV receives mostly information from neurons that sense mechanical pressure and laminae V and VI are in general handed information about joint angle, muscle length, and muscle tension. Most nociceptive primary afferents terminate in laminae I and II, but some reach the deeper laminae (Sugiura *et al.* 1986). For review see (Todd 2002).

The postsynaptic cells can be classified into three main groups: interneurons, propriospinal neurons and projection neurons. Interneurons remain in the gray matter of the spinal cord and can be divided into two main classes; excitatory (glutaminergic) and inhibitory (γ-aminobutyric acid (GABA)-ergic and/or glycinergic). The propriospinal neurons connect the different levels in the spinal cord in addition to connect the contralateral and ipsolateral

side. The projection neurons have long axons that usually cross the midline and travel rostrally in the contralateral white matter to terminate in various higher brain areas. For review see (Todd 2010).

Projection neurons relevant for pain can be classified as either nociceptive specific (NS) neurons or wide dynamic range (WDR) neurons. NS neurons are primary located superficially and receive nociceptive input only. The WDR neurons are located in the deeper lamina and receive both noxious and innoxious input. They thereby respond to the whole spectra of mechanical, thermal and chemical stimuli. For review see (Hoffman *et al.* 1981).

1.4.2 Ascending pathways and descending modulation

Information to the somatosensory cortex, regarding pain intensity and localization is conveyed via the thalamus from projection neurons in lamina V, providing the sensory-discriminative aspects of pain. Information from projection neurons in lamina I and II travel to the parabrachial area, hypothalamus, periaqueductal gray (PAG), amygdala, insula and cingulated cortex. These areas are involved in the unpleasant feeling, fear and anxiety, as well as autonomic activation and homeostatic regulation relating to pain, thus providing the affective-motivational aspect of pain. For review see (Gauriau and Bernard 2002).

PAG, pons and rostroventral medulla are important structures that control the activity in the serotonergic, noradrenergic and enkephalinergic descending projections, which modulate the neuronal transmission in the spinal cord. PAG receives information from the prefrontal cortex, insula, lateral hypothalamus and the amygdala in addition to receive information from ascending sensory pathways. The descending modulatory system can therefore be influenced by complex cognitive and emotional processes, and the dorsal horn can act as a filter for nociceptive signaling controlled by the pain modulatory system in the brain. For review see (Gjerstad 2007).

Taken together, the pain experience is a product of nociceptive signaling as well as emotional and cognitive processes. An anatomical overview of the signaling system between the dorsal horn and the brain is illustrated in figure 1.4.

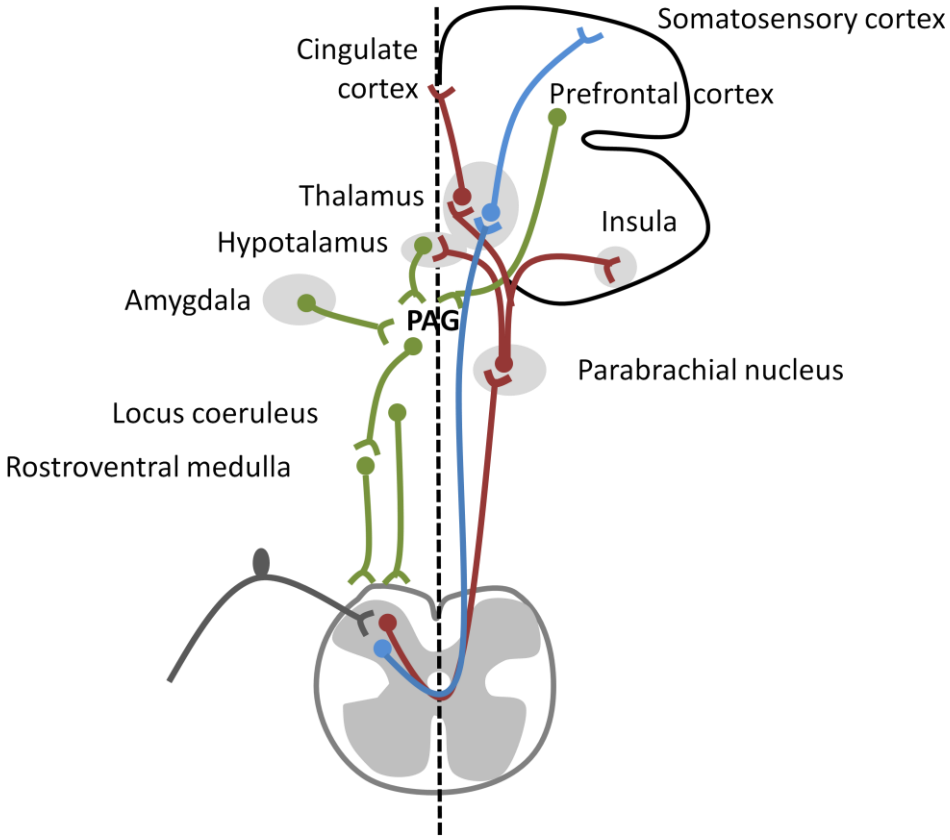

Figure 1.4: Anatomy of the pain signaling system from the dorsal horn to the brain. Projection neurons from the dorsal horn can take two routes to the brain. Route one (blue) includes projection neurons from lamina V, which sends information to the thalamus and further to the somatosensory cortex, giving information about the location and intensity of painful stimuli. Projection neurons in lamina I and II (red) sends information to the parabrachial nucleus. From the parabrachial nucleus the signals are conveyed to insula, amygdala, thalamus, hypothalamus and cingulated cortex, which are areas connected with emotion such as fear and avoidance. Descending pathways (green) carries information from hypothalamus and amygdala through PAG, via either the locus coeruleus (noradrenergic descending projections) or the rostroventral medulla (serotonergic or enkephalinergic descending projections), and modulates transmission in the spinal cord. The dorsal horn is therefore acting as a filter for nociceptive signaling which is controlled by the pain modulatory system in the brain. PAG: Periaqueductal gray. Adapted from (Gjerstad 2007).

1.4.3 Sensitization

Injury, inflammation and nerve damage sensitize primary afferent nerve fibres and enhance the nociceptive neurotransmission. According to IASP the definition of sensitization is an increased responsiveness of nociceptive neurons to their normal input, and/or recruitment of a response to normally sub-threshold inputs. Peripheral sensitization involves a reduced threshold of nociceptive neurons in the periphery to stimulation of their receptive fields, whereas central sensitization refers to increased responsiveness of nociceptive neurons in the CNS to their normal or sub-threshold afferent input.

Mild noxious stimulation of the nociceptive fibres will result in the release of Glutamate (Glu) from primary afferent fibres. Glu activates the α-amino-3-hydroxy-5-methyl-4-isoxazolepropionic acid (AMPA) receptor, which results in an inward positive current and a transient depolarization. If the stimulation is more intense or prolonged it may result in the co-release of Glu and SP from the primary afferent fibres. This release leads to the activation of AMPA, metabotropic glutamate (mGlu) and neurokinin-1 (NK1) receptors, which again leads to a more substantial depolarization and activation of T-type Ca^{2+} channels and removal of the voltage gated Mg^{2+} blockade of the N-methyl-D-aspartate (NMDA) receptors. Glu binds to unblocked NMDA receptors and will together with T-type Ca^{2+} receptor allow substantial Ca^{2+} influx into the postsynaptic cell. Activation of mGlu and NK1 receptors induces phospholipase C (PLC) to engage inositol 1,4,5-triphosphate (IP_3) which mediates Ca^{2+} release from intracellular stores. For review see (Latremoliere and Woolf 2009).

An increased concentration of cytosolic Ca^{2+} will activate many Ca^{2+}-dependent enzymes, including Ca^{2+}-calmodulin dependent kinase II (CAMKII) (Pedersen *et al.* 2005), protein kinase A (PKA) (Lin *et al.* 2002) and extracellular signal related kinase (ERK) (Rosen *et al.* 1994; Xu *et al.* 2008). All these proteins phosphorylates different target proteins and initiate several intracellular signaling cascades leading to post-translational, translational and transcriptional changes. These changes can cause an enhanced synaptic efficacy. One example is that phosphorylation of AMPA receptors and NMDA receptors can cause enhanced channel opening time and conductance (Carvalho *et al.* 2000; Chen and Roche 2007).

In addition to neurons the CNS also contains glia cells, which gives important biochemical support. Microglia, one type of glia cells, can upon activation function as specialized immune cells. They express the IFN-γ receptor and binding of IFN-γ may activate microglia. Once activated, microglia can produce cytokines and neurotrophic factors that can influence the neuronal processes and lead to hyperexcitability in the dorsal horn and long-lasting pain hypersensibility (Tsuda *et al.* 2009). Hence, microglia may play an important role in central sensitization after injury. For review see (Watkins *et al.* 2001).

Sensitization of nociceptive nerve endings rarely outlasts the primary cause for pain and is usually restricted to the area of injury and is therefore considered adaptive. Central changes, in contrast, may outlast the initial trigger and spread to sites remote from the primary cause of pain. Central sensitization may therefore be a precursor for development of chronic pain after disc herniation. For review see (Cervero 1995).

Nucleus pulposus and sensitization

Mechanical compression of the nerve root, by the displaced disc material, may be associated with lumbar radicular pain after disc herniation (Winkelstein *et al.* 2002). In addition, the inflammatory processes induced by contact between NP tissue and neuronal tissue may also be important (Olmarker *et al.* 1995).

When NP is applied onto DRG, or nerves entering the spinal canal, it induces structural and functional changes in the nerve roots (Olmarker *et al.* 1993). These changes include sensitization of dorsal horn neuronal responses (Takebayashi *et al.* 2001; Anzai *et al.* 2002; Cuellar *et al.* 2005), attraction of immune cells (Ikeda *et al.* 1996) and reduction of blood flow in the DRG (Yabuki *et al.* 1998). In behavioral studies NP has also been shown to cause mechanical- and thermal hyperalgesia (Kawakami *et al.* 1996), as well as spontaneous pain (Olmarker 2008).

A number of pro-inflammatory cytokines, as well as other mediators, have been identified in or around the herniated disc. Some of these substances may be released from NP cells, while others may be released from attracted immune cells. TNF-α (Olmarker and Larsson 1998), IL-1β (Le Maitre *et al.* 2005), IL-6 (Rand *et al.* 1997) and IFN-γ (Tanga *et al.* 2005) has been suggested to be involved because of their neurotoxic properties. For review see (Risbud and Shapiro 2014).

These inflammatory substances may increase the sensitivity of the nerve roots and induce sensitization at the spinal level. Several animal studies have reported pain behavior following injections of pro-inflammatory cytokines (DeLeo *et al.* 1996; Wagner and Myers 1996; Murata *et al.* 2006). Moreover, administration of pro-inflammatory cytokine blockers after peripheral nerve injury or inflammation reduces the pain response to noxious stimuli (Sommer 1999; Nakamae *et al.* 2011). In addition, electrophysiological recordings have shown that cytokines may increase the neuronal excitability through direct or indirect interaction with receptors and ion channels. For review see (Schafers and Sorkin 2008).

Afferent fibres, DRG cell bodies, spinal cord neurons and glia cells express cytokine receptors. Therefore, pro-inflammatory cytokines released after disc herniation may induce low back pain and sciatica through influencing nociceptors close to the intervertebral disc nerve roots and DRG.

An overview of the signaling cascade after stimulation of primary afferent fibres and the effects of NP on spinal nerves is illustrated in figure 1.5.

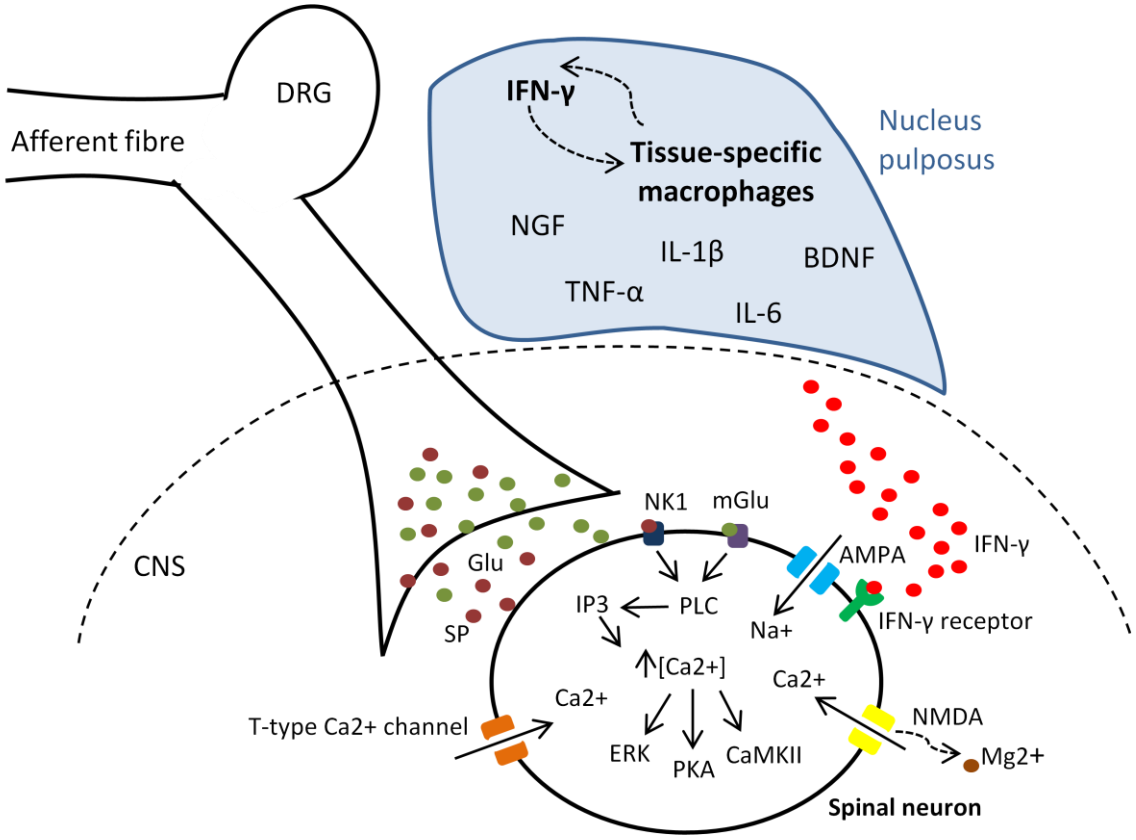

Figure 1.5: The effect of nucleus pulpous on neurons in the spinal dorsal horn. Afferent fibres terminate in the dorsal horn where they synapse with spinal neurons. Mild noxious stimulation will result in release of Glu from the pre-synaptic cell. More intense or prolonged stimulation can lead to a co-release of Glu and SP. Glu activates AMPA receptors, which results in an inward positive current and a transient depolarization. Glu also activates mGlu receptors which, through PLC and IP3, increase the intracellular Ca^{2+} concentration by mediating calcium release from intracellular stores. The NK1 receptor, which binds SP, also leads to an increase in cytosolic Ca^{2+} through the same pathway. A depolarization will activate the T-type Ca^{2+} channels, causing an influx of calcium ions, and combined with the activation of NK1- and mGlu receptors a more substantial depolarization. This will remove the Mg^{2+}-block from the NMDA receptors. Glu can bind to unblocked NMDA receptors, and activated NMDA receptors allows Na^{+} or Ca^{2+} to move into the cell, or K^{+} to move out of the cell in a voltage dependent manner. Elevated intracellular Ca^{2+} concentration leads to activation of several calcium dependent enzymes ultimately leading to phosphorylation of different target proteins, which results in post-translational, translational and transcriptional changes. Pro-inflammatory cytokines released from NP after disc herniation, such as TNF-α, IL-1β, IL-6 and IFN-γ, as well as neurotrophins such as BDNF and NGF have been thought to be involved in this sensitization mechanism by influencing ion channels and/or gene expression. The dotted line indicates the meninges and thus the separation between the CNS and the periphery. AMPA: α-Amino-3-hydroxy-5-Methyl-4-isoxazolepropionic Acid; BDNF: Brain-Derived Neurotrophic Factor; CAMKII: Ca^{2+}-Calmodulin dependent Kinase II; CNS: Central Nervous System; DRG: Dorsal Root Ganglion; ERK: Extracellular signal Related Kinase; Glu: Glutamate; IFN-γ: Interferon-γ; IL-1β; Interleukin-1β; IL-6: Interleukin-6; IP3: Inositol 1,4,5-Triphosphate; mGlu: metabotropic Glutamate receptor; NGF: Nerve Growth Factor; NK1: Neurokinin-1 receptor; NMDA: N-Methyl-D-Aspartate; NP: Nucleus Pulposus; PKA: Protein Kinase A; PLC: Phospholipase C; SP: Substance P; TNF-α: Tumor Necrosis Factor-α.

IFN-γ and sensitization

In addition to being a key regulator in the immune system and inflammation, IFN-γ may inhibit glutamate receptor 1 (GluR1) positive interneurons and have a neurotoxic effect. The IFN-γ receptor forms a unique, neuron-specific, calcium-permeable receptor complex with AMPA receptor subunit GluR1. Through this receptor IFN-γ phosphorylates GluR1 by the aid of JAK1-2/STAT1 pathway and PKA. This leads to an increase in Ca^{2+} influx and nitric oxide (NO) production, which in turn will lead to a decrease in ATP production (Mizuno *et al.* 2008). Hence, IFN-γ enhances AMPA-induced neurotoxicity, which can lead to a neuronal dysfunction.

GluR1 can almost exclusively be found on inhibitory interneurons, while GluR2 can be found on excitatory interneurons (Kerr *et al.* 1998). After treatment with IFN-γ it has been suggested that the dorsal horn neuronal network has been sensitized (Vikman *et al.* 2003). It is therefore believed that the activation of JAK1-2/STAT1 pathway may induce a long lasting depolarization and have a neurotoxic effect primary on the inhibitory interneurons. At the spinal cord level this leads to disinhibition and increase in nociceptive signaling. Moreover, GluR1 is mainly found in a sub-population of neurons located in the spinal cord laminae I and II. This localization suggests that IFN-γ may modulate the processing of nociceptive information in this region (Popratiloff *et al.* 1996).

In addition, increased cytosolic concentration of calcium ions and the subsequent increase in NO production can affect neurons close to the inhibitory interneurons. NO is a signal molecule that has been shown to regulate neuronal excitability, but also have a neurotoxic effect in large concentrations. For review see (Calabrese *et al.* 2007).

An overview of the IFN-γ effect on spinal interneurons is illustrated in figure 1.6.

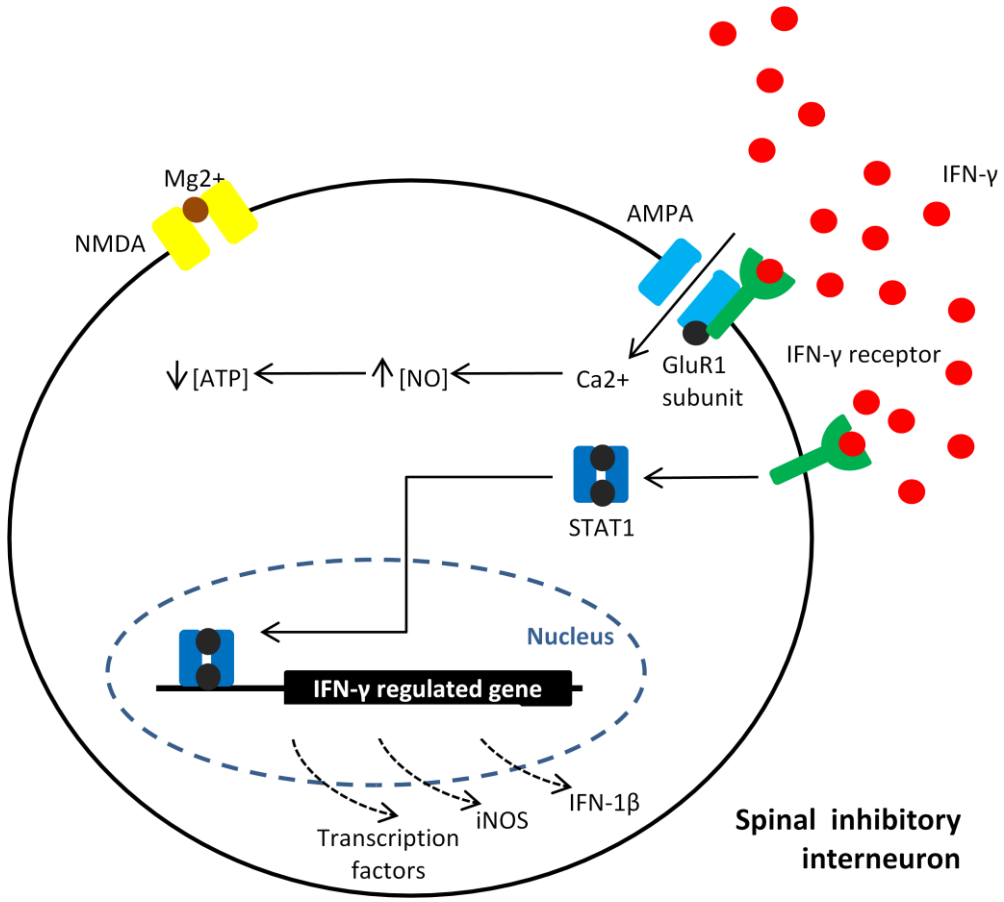

Figure 1.6: The effect of IFN-γ on spinal inhibitory interneurons. The IFN-γ receptor forms a calcium permeable receptor complex with the AMPA subunit GluR1, leading to an increased Ca^{2+} influx and long lasting depolarization. This subsequently leads to an increase in NO production and decrease in ATP concentration. IFN-γ thereby enhances AMPA-induced neurotoxicity, leading to neuronal dysfunction of the inhibitory interneurons and central sensitization. Activation of the IFN-γ receptor can also lead to phosphorylation and activation of STAT1 and production of IFN-γ regulated genes, such as transcription factors for other inflammatory mediators, iNOS and IFN-1β. AMPA: α-Amino-3-hydroxy-5-Methyl-4-isoxazolepropionic Acid; ATP: Adenosine-Tri-Phosphate; GluR1: Glutamate Receptor 1; IFN-γ: Interferon-γ; IFN-1β: Interferon-1β; iNOS: inducible Nitric Oxide Synthase; NMDA: N-Methyl-D-Aspartate; NO: Nitric Oxide; STAT1: Signal Transducer and Activator of Transcription 1.

1.5 Genetics

A number of factors are thought to serve as primary initiating events that lead to the abnormal production of cytokines by the intervertebral disc. These factors include genetic predisposition, smoking, infection, mechanical trauma, as well as aging.

Although humans are similar in terms of the genome, we are not identical. Small differences in the deoxyribonucleic acid (DNA) sequence among individuals account for the heritable phenotypic variations in the population. It is these variations in the DNA sequence that decide our susceptibility for various diseases, including predisposition for chronic pain. For review see (Brookes 1999).

Many of the genes in the human DNA are polymorphic, meaning that they exist in multiple variants. Substitution of a single base pair (bp) is the most frequently occurring type of genetic variability. Such variants are called single nucleotide polymorphisms (SNPs) and occur approximately every 300bp (Kruglyak and Nickerson 2001). Other types of variants include short insertions or deletions and variable number of tandem repeats. These polymorphisms, depending on their localization, may influence the rate of transcription, stability of messenger ribonucleic acid (mRNA) or the activity of the resulting protein.

Substitution of a base pair can be categorized into two main groups; coding and non-coding SNPs. The coding SNPs fall within the coding sequence of a gene and can either be a non-synonymous SNP, leading to a change in the amino acid composition of the protein or a synonymous SNP which does not change the amino acid composition. A protein can be fully functional with an amino acid substitution, but a change can also lead to a non-functional protein or a change in protein function, which can lead to disease. SNPs in non-coding regions may affect the gene expression through regulation, including splicing, regulation of transcription factors and regulation of microRNA target sites. The non-coding SNPs can be found either in front or behind the coding region of the gene, in the introns, in intrinsic regions or in pseudogenes.

1.5.1 Single Nucleotide Polymorphisms in IFN-γ

Many SNPs for IFN-γ has been described in different regions of the gene, some of which are depicted in figure 1.7.

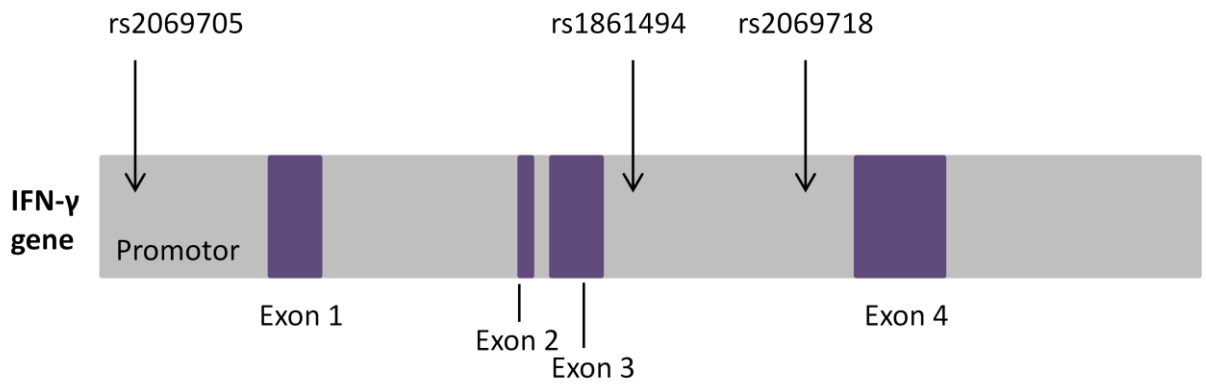

Figure 1.7: A schematic overview of relevant SNPs in the IFN-γ gene. SNP rs2069705 is located in the promoter and rs1861494 and rs2069718 is located in intron 3. Purple indicates exons, whereas gray indicates introns or promoter/untranslated 3' end. IFN-γ: Interferon-γ; SNP: Single Nucleotide Polymorphism.

In general, the promoter is important for the gene expression. The SNP rs2069705 is located in the IFN-γ promoter. It has been indicated that the SNP may be associated with the susceptibility for systemic lupus erythematosus (SLE) (Kim *et al.* 2010). SLE is a disease with a pathogenesis involving excessive production of IFN-γ (Harigai *et al.* 2008). It is therefore likely that the promoter SNP may be associated with transcription rate of the gene and thereby IFN-γ expression level.

The non-coding introns can also affect the gene expression. For example, intron 3 has previously been indicated to possess enhancer activity as well as contain a T-box binding element, indicating that SNPs in this area may be important for the transcription (Li-Weber and Krammer 2003). It has been suggested that the wild-type allele (T) for rs1861494, in intron 3, has a higher binding affinity for nuclear factors than the C allele (Kumar and Ghosh 2008). Since CCAAT/Enhancer binding protein-β (CEBPB) has its binding site where the SNP is located, the SNP may influence the binding of the enhancer protein. CEBPB is important in the regulation of many cytokine genes involved in the acute phase of the inflammatory response.

In addition rs2069718, another intron 3 SNP, have been thought to be associated with SLE (Kim *et al.* 2010), suggesting that the SNP may also influence the IFN-γ gene expression.

2 Aims

The purpose of this master project was to provide new knowledge about the relationship between genetic factors and development of lumbar radicular pain following disc herniation. First, the relevant genes were defined by an animal model mimicking the clinical situation after intervertebral disc herniation. In addition, the relationship between genetic polymorphisms in one of these genes and pain in sciatica patients was studied. Five sub goals were defined:

I. Examine the changes in gene expression in NP tissue exposed to the spinal dorsal nerve roots for one hour by:

    a. Performing a PCR array screening to determine possible up-regulated candidate genes in NP.

    b. Follow-up analysis of candidate genes by qPCR.

II. Examine if the inflammatory process includes macrophage infiltration into NP.

III. Confirm that application of NP tissue from herniated discs onto the dorsal nerve roots for one hour may enhance the spinal neuronal activity.

IV. Investigate if application of the most relevant pro-inflammatory protein (determined in aim I) onto the dorsal nerve roots mimics the effect of NP.

V. Observe if genetic polymorphisms in the most relevant pro-inflammatory cytokine (determined in aim I and IV) may be associated with acute pain and disability following disc herniation in sciatica patients.

3 Materials and methods

3.1 The animal study

All animal experiments were approved by the Norwegian Animal Research Authority (NARA). The experiments were performed in accordance with the European Convention for the Protection of Vertebrate Animals used for Experimental and Other Scientific Purposes.

3.1.1 Animal handling

The experiments were performed on genetic identical female Lewis rats (Harlan Laboratories Inc., UK) weighing between 165 and 206 grams. The animals were housed at room temperature in groups of four in the animal facility at the National Institute of Occupational Health, with free access to food and water. After arrival the animals were acclimatized for at least 5 days. The animals were sacrificed immediately after the experiments.

3.1.2 Surgery

The animals were sedated with isoflurane gas (Baxter International Inc., USA) for approximately one minute, and anesthetized with intraperitoneal administration of urethane (Sigma-Aldrich Co., USA) with a concentration of 250 mg/ml. Urethane (1.8-2.7 mg/g bodyweight) was administrated with several small injections to avoid overdose. Absence of foot withdrawal and ear reflexes indicated adequate surgical anesthesia.

The rats were shaved to get better access during surgery. Simplex (80 % Vaseline and 20 % paraffin) was applied to prevent the eyes from drying. The core temperature of the animal was monitored by a feedback heating pad (homeothermic blanket control unit, Harvard Apparatus Ltd. Kent, UK) set on 36-37°C.

A section of the sciatic nerve was dissected free and isolated from the surrounding tissue using parafilm. Two ear bars attached to the frame were used to stabilize the head. A laminectomy was performed on vertebrate Th13-L1, corresponding to the spinal cord segments of L3-S1, where the sciatic nerve roots enter the spinal cord. The vertebral column was fixed with clamps, both rostral and caudal to the exposed spinal cord. The meninges (dura mater and arachnoidea) were carefully removed before the experiment started.

3.1.3 Investigation of gene expression in NP tissue

The NP tissue was harvested from 3-5 tail vertebrae of a genetic identical donor rat. Following ribonucleic acid (RNA) isolation the quantity and quality was measured and complimentary DNA (cDNA) was made. A screening regarding 84 common cytokine genes was performed, and genes of interest were determined. Primers were designed and quantitative polymerase chain reaction (qPCR) was run to determine the fold expression in the genes of interest. An outline of the gene expression study can be viewed in figure 3.1.

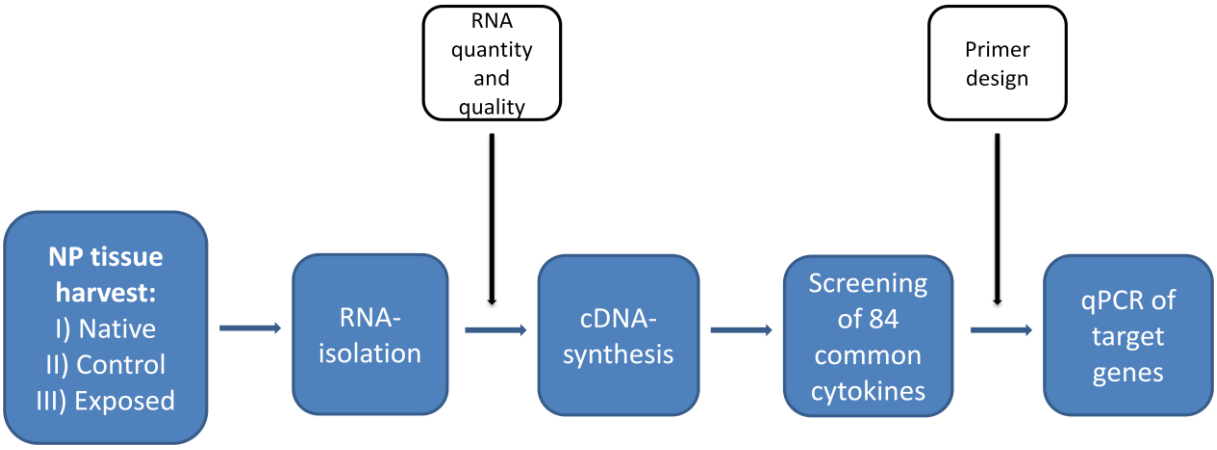

Figure 3.1: Protocol of the gene expression study. cDNA: complimentary DNA; NP: Nucleus Pulposus; qPCR: quantitative Polymerase Chain Reaction.

Tissue harvesting

The gene expression of the harvested NP tissue was investigated in three different groups: I) Native, II) Control and III) Exposed. After the experiments the tissue was frozen in liquid nitrogen. NP from the native group was frozen directly after harvesting. The tissue in the control and exposed group were bisected from the same donor rat. NP tissue in the control group was kept in 0.9 % NaCl at room temperature, while NP tissue in the exposed group was applied onto the spinal dorsal nerve roots. After 60 minutes the tissues were frozen. The timeline is illustrated in figure 3.2.

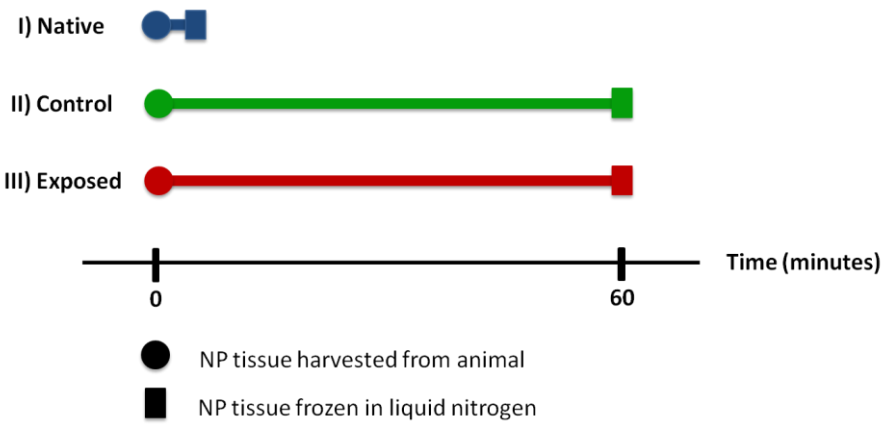

Figure 3.2: Protocol for tissue harvesting from nucleus pulposus. The blue timeline indicates the native tissue. The green timeline indicates the control in 0.9 % NaCl. The red timeline indicates the tissue exposed for dorsal nerve roots. The circle indicates when the NP tissue was harvested from the donor rat and the square indicates when it was frozen. NP: Nucleus Pulposus.

RNA isolation and cDNA synthesis

Isol-RNA lysis Reagent (5 PRIME) was added to the NP tissue. Three sterile metal balls were added to each sample and the tissue was homogenized by aid of a mixer mill (Retsch MM 301, Haan, Germany). After incubation and centrifugation the supernatant was transferred to a new eppendorf tube, thereby removing all non-solubilised cell material. Chloroform was added to separate the mixture into three phases, one water phase containing RNA, one phase containing DNA and protein, and one isol-phase containing a mixture of lipids and proteins. The upper water phase was transferred into a new eppendorf tube, where isopropanol was added. The resulting RNA pellet was washed with 75 % ethanol, dried, and at last resuspended with RNase free water. The concentration of the RNA solution was established using a NanoDrop 8000 Spectrophotometer (Thermo Scientific, USA). The RNA was further diluted with RNase free water to a concentration of 250 ng/µl. The protocol can be found in appendix 1.

The quality of the RNA was evaluated with on-chip electrophoresis using an Agilent 2100 Bioanalyzer and an Agilent RNA 6000 Nano Kit (Agilent Technologies, Waldbonn, Germany). RNA from two and two samples was mixed together before testing. During the electrophoresis ribosomal subunits, S18 and S28, were separated by the bioanalyzer and the RNA was detected using fluorescence. An electrophoresogram for each sample added to the chip was made. RNA of high quality would show two peaks close together at approximately 40 and 50 s. A RNA integrity number (RIN)-value was calculated by the software from the electropherogram. Totally degraded RNA was indicated by a RIN-value of 1, whereas

perfectly intact RNA was indicated by a RIN-value of 10. All the samples had a RIN-value over 6.4, which were considered satisfactory. The protocol can be found in appendix 2.

A first strand cDNA synthesis kit for reverse-transcriptase qPCR (Roche Diagnostics, Mannheim, Germany) was used to reversely transcribe the mRNA into cDNA. Firstly, random primer, deoxynucleotide mix and 1.5 µg RNA was incubated at 65°C in a denaturation step. Next, reaction buffer, $MgCl_2$, RNase inhibitor and AMV reverse transcriptase were added to transcribe the mRNA to cDNA. The cDNA reaction was carried out in a Perkin Elmer Cetus DNA Thermal Cycler 480 on the following program: 42°C for 60 minutes, 99°C for 5 minutes and 4°C for 5 minutes. The cDNA was diluted with tri-ethylenediaminetetraacetic acid (TE)-buffer to a final concentration of 10 ng/µl and stored at -80°C. For protocol see appendix 3.

qPCR

A Rat Common cytokines RT^2 Profiler PCR Array (Qiagene, Cat. no. 330231 PARN-021ZA) with 84 common cytokine genes was used to investigate the gene expression in exposed tissue after 60 minutes compared to the native samples. In addition to the cytokine genes, several house-keeping genes were present at the array. Two pooled cDNA screening sample mixes containing I) all the samples from the exposed NP tissue and II) all the samples from the native NP tissue, were prepared and mixed together with water and SYBR Green mastermix. The PCR components mix was dispensed into the PCR array. A plastic film was used to seal the array before centrifuging for 1 minute at 1000g to remove bubbles. The PCR array run was performed in a StepOnePlus cycler (Applied Biosystems, California, USA) at the following program: 10 minutes at 95°C and 40 cycles with 15 seconds at 95°C and 1 minute at 60°C. For protocol and array set-up see appendix 4.

IL-1β, a known up-regulated cytokine, was used as a positive control. Cycle threshold (C_t)-value over 30, indicating an unreliable low concentration in the sample, was used as an exclusion criterion.

The up-regulation ($\Delta\Delta C_t$, indicating fold change) shown in the PCR array was calculated from a data-sheet downloaded from Qiagene using the following equation:

$$\Delta\Delta C_t = (\Delta C_{t\ Exposed}) - (\Delta C_{t\ Native}), \text{ where } \Delta C_t = \Delta C_{t\ target\ gene} - \Delta C_{t\ \beta\text{-actin}}$$

Based on the PCR array genes of interest were defined and primes were designed using Primer Express 2.0 (Applied Biosystems, California, USA). The primers were delivered from DNA technology (Risskov, Denmark). To avoid amplification of genomic DNA and non-specific secondary structures the primers were designed to span introns. The primers specificity was also checked by performing a BLAST search.

From the PCR array Interferon-γ (IFN-γ), Interferon-α2 (IFN-α2), Interferon-1β (IFN-1β) and Interferon-α4 (IFN-α4) were selected for a follow-up analysis with qPCR. β-actin was used to normalize the gene expression. The sequences can be viewed in table 3.1. All samples were tested in parallels.

Table 3.1 Primers used for qPCR

Primer	Sequence (5'→3')	Tm (°c)	GC-content (%)
Interferon-γ forward	TCCAATCGCACCTGATCACTAA	59	45
Interferon-γ reverse	GGGTTGTTCACCTCGAACTTG	58	52
Interferon-1β forward	TTGCGTTCCTGCTGTGCTT	59	53
Interferon-1β reverse	TCGGAACTGGAGCTGCTTGT	60	55
Interferon-α2 forward	AGCTATCCCCTGTCCTGCATGA	58	52
Interferon-α2 reverse	GAATGAGTCTAGCAGGATGCAT	58	48
Interferon-α4 forward	GGCTCAAACCATCCCTGTTC	58	55
Interferon-α4 reverse	TCCAAGCAGCAGATGAGTCCTT	60	50
Interleukin-1β forward	CGTGGAGCTTCCAGGATGAG	59	60
Interleukin-1β reverse	CGTCATCATCCCACGAGTCA	59	50
β-Actin forward	CTAAGGCCAACCGTGAAAAGA	58	48
β-Actin reverse	ACAACACAGCCTGGATGGCTA	59	52

A: Adenosine; C: Cytosine; G: Guanine; GC-content: Guanine/Cytosine-content; T: Tyrosine; Tm: melting temperature.

The qPCR reaction was performed on the StepOnePlus cycler (Applied Biosystems, California, USA) at the following program: 2 minutes at 95°C and 40 cycles with 10 seconds at 95°C and 30 seconds at 60°C. StepOne Software 2.3 was used to analyze the data. For protocol see appendix 5.

SYBR Green, the fluorescence reporter used during the qPCR measurements, is an unspecific double stranded intercalating dye that gives out fluorescence at 520 nm when incorporated in the DNA. This means that SYBR Green can bind to any amplified DNA, primer dimers and other unspecific products in the reaction mixture. This could be a problem in the quantification since it is only the total amount of fluorescence that is measured during qPCR. To verify the specificity in the qPCR run, a melting curve of fluorescence vs. temperature was created and analyzed. An ideal qPCR run would only contain a single peak in the melting curve, as any additional peaks would indicate a co-amplification of other products. Runs containing more than one peak were eliminated from further study.

A standard curve was constructed for each run, both target gene and β-actin. It was constructed in a fourfold dilution series from random samples. This type of dilution gives a theoretically C_t distance of two cycles between each sample in the standard curve. Using the C_t-values and the standard curve the amount of RNA converted to cDNA in the original sample was established. Raw data examples are shown in figure 3.3.

(A)

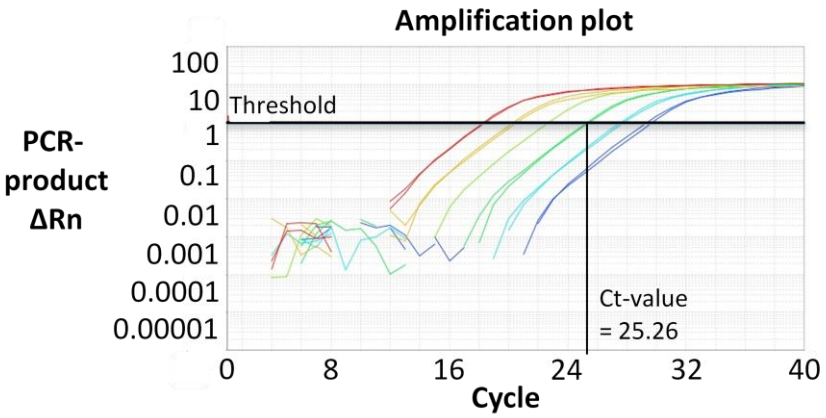

(B)

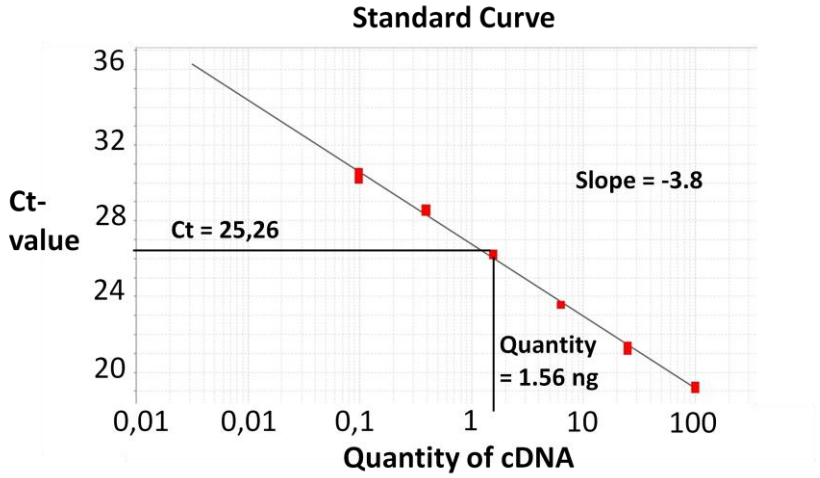

(C)

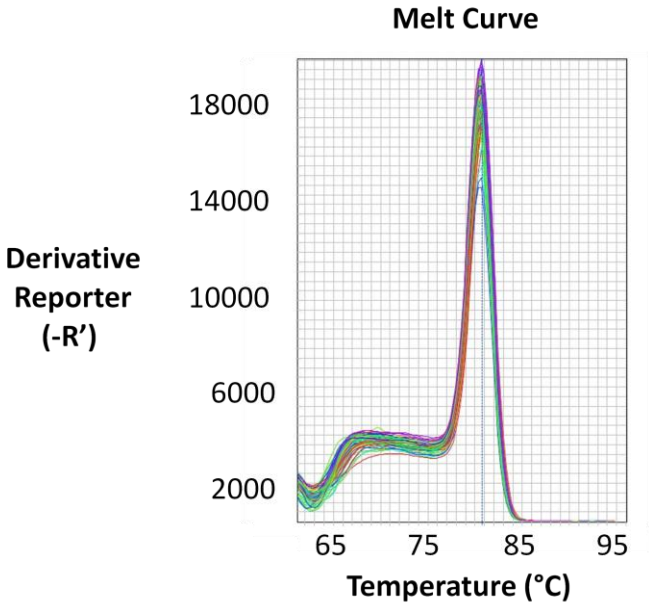

Figure 3.3: qPCR on nucleus pulposus tissue. A) Amplification plot of a dilution series on a β-actin run, illustrating C_t-value and an approximate two cycle distance between each sample. B) Standard curve drawn from the dilution series. It is also indicated how a C_t-value is calculated into quantity of cDNA. C) Example melt curve, a uniform top indicates one PCR product.

3.1.4 Macrophages in NP tissue

To investigate the possibility of macrophages in NP tissue primers were designed for CD68 and F4/80, known biomarkers for macrophages. The primers were designed using Primer Express 2.0 as previously described, and the sequences are listed in table 3.2. qPCR was performed and the results analyzed with regards to the same criteria as in the gene expression study. The β-actin primers were the same as for the gene expression study (table 3.1).

Summary of the protocol in illustrated in figure 3.1.

Table 3.2 Primers used for qPCR

Primer	Sequence (5'→3')	Tm (°c)	GC-content (%)
CD68 forward	CTCACAAAAAGGCTGCCACTCT	60	52
CD68 reverse	TTCCGGTGGTTGTAGGTGTCT	58	58
F4/80 forward	GGGCAAGGCCGGAATCT	59	65
F4/80 reverse	GGATGGTAAAGGTGGCATTCA	58	48

A: Adenosine; C: Cytosine; G: Guanine; GC-content: Guanine/Cytosine-content; T: Tyrosine; Tm: melting temperature.

3.1.5 Electrophysiological extracellular single cell recordings

As previously described (Egeland *et al.* 2013) a laminectomy was performed before a bipolar silver hook electrode (1.5 mm distance between hooks) was placed proximal to the main branches of the sciatic nerve for electrical stimulations. A parylene-coated tungsten microelectrode (impedance 2.0 to 4.0 MΩ) (Fredrick Haer & Co., Bowdoinham, ME, USA) was lowered vertically into the left dorsal horn of the spinal cord by an electrically controlled micromanipulator (Märzhäuser Wetzlar GmbH & Co. KG, Wetzlar, Germany). A reference electrode was placed subcutaneously.

With the help of the electrode, spinal cord segments L3-S1 were identified by the neuronal responses to left hind paw stroking and pinching. The neuronal activity was monitored acoustically by the help of a loud speaker and visually by a graphic display on the computer to ensure correct location in the spinal cord. The signals were filtered with a half amplitude cutoff, so only frequencies between 500 and 1250 Hz (corresponding to the wavelength of 0.8-2 ms) could be detected.

From depths between 50 to 400 µm from the spinal cord surface single cell potentials were recorded. The recorded signals were captured with a headstage and amplified (x5000) with an AC pre-amplifier, band-pass filtered (NeuroLog by Digitimer Ltd, Hertfordshire, UK), before digitalized with the interface CED Micro1401. All the data were stored by the software CED Spike 2.2 (Cambridge Electronic Design, Cambridge UK).

Electrical stimuli to the sciatic nerve by the hook electrode were controlled by the software Spike 2.2 and interface CED Micro1401. The intensity of the stimuli was controlled by a pulse buffer connected to a stimulus isolator unit (NeuroLog by Digitimer Ltd, Hertfordshire, UK).

A schematic overview of the experimental set-up is illustrated in figure 3.4.

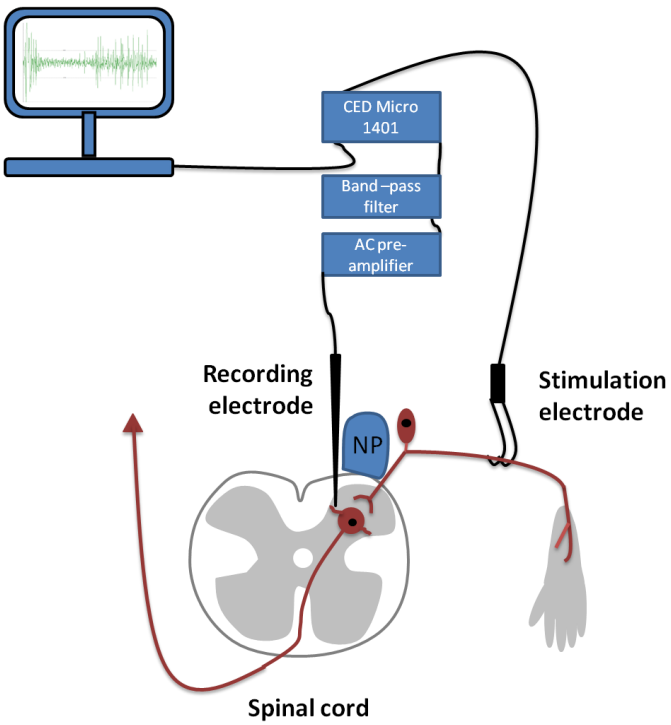

Figure 3.4: The experimental set-up for electrophysiological recordings. A schematic overview of the experimental set-up for electrophysiological single cell recordings in the spinal dorsal horn. Signal from the spinal cord was amplified with an AC pre-amplifier and filtered with a band-pass filter, before digitalized with CED micro 1401 interface. Stimulations to the sciatic nerve via a hook electrode were controlled by the interface and the Spike 2.2 software. The software also stored all data. NP: Nucleus Pulposus

At the start of each experiment a C-fibre threshold was defined as the lowest stimulus intensity that evoked a visible C-fibre response (figure 3.5A). Throughout the experiment a single test stimulus (2-ms rectangular pulse, 1.5 x C-fibre threshold) was delivered every 4th minute to the left sciatic nerve.

(A) **(B)**

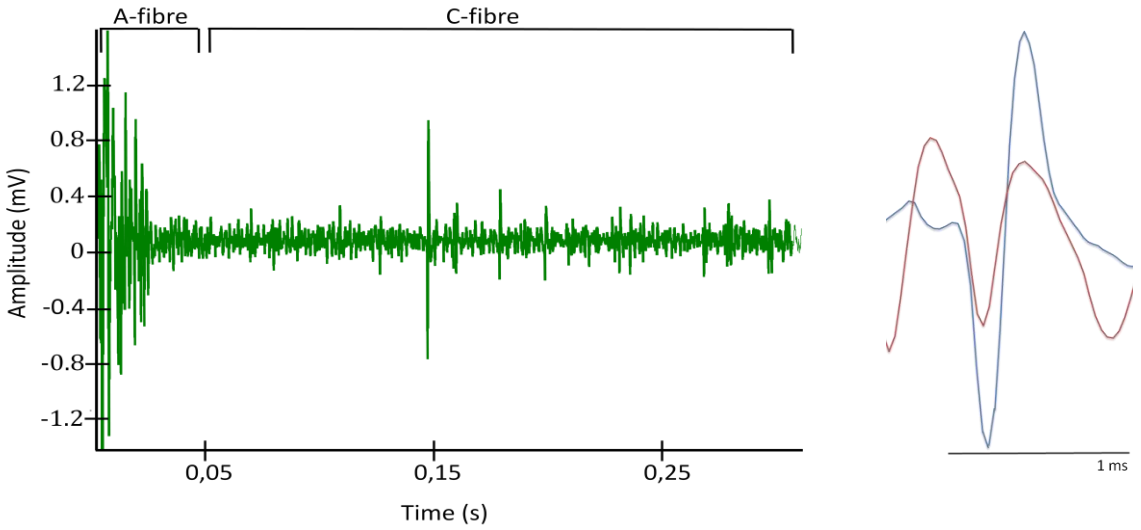

Figure 3.5: Neuronal activity monitored visually by a graphic display on the computer. A) By the help of the graphics on the computer A- and C-fibre responses were separated on the basis of latencies. A spike between 50 and 300 ms was defined as C-fibre. A response to a test stimulus where only one C-fibre spike was visible was used to define threshold. B) An illustration of how shape and amplitude can separate two cells in a single cell recording.

By the help of the graphics on the computer, A- and C-fibre responses were separated on the basis of latencies, where a spike between 50 and 300 ms was defined as a C-fibre response. To ensure single cell recording the amplitude and shape of the spikes were carefully analyzed (figure 3.5B).

Before a recorded experiment could begin, a baseline had to be defined. Six stable C-fibre responses to a test stimulus, with a variance under 20 %, would qualify as a baseline.

A timeline for the different groups in the electrophysiological experiments is illustrated in figure 3.6.

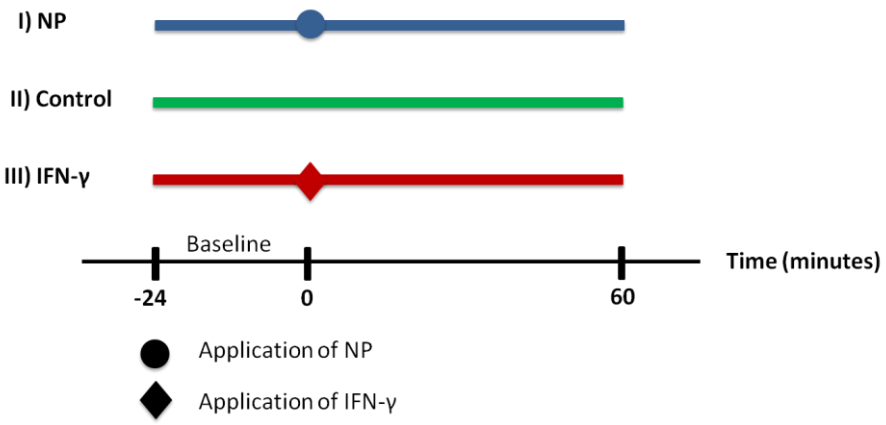

Figure 3.6: Protocol for the electrophysiological experiments. Blue indicates the timeline for NP experiments and the circle indicates the time point for application of NP onto the spinal dorsal nerve rots. The green timeline indicates the protocol for the control experiments where only 0.9 % NaCl was administrated during the recordings. The red timeline indicates the protocol for IFN-γ experiments. The diamond indicates when IFN-γ was administrated onto the spinal dorsal nerve roots. IFN-γ: Interferon-γ; NP: Nucleus Pulposus.

NP application

NP was harvested from 3-5 tail vertebrae of a genetic identical donor rat and applied caudally of the recording electrode on the spinal cord to cover the incoming spinal dorsal nerve roots after baseline was recorded. The C-fibre responses were followed for one hour after NP application.

INF-γ administration

1000 U recombinant IFN-γ from rat made in E.coli (Calbiochem, Merck Millipore, Nottingham, UK) in a total volume of 25 µl was applied onto the spinal dorsal nerve roots after baseline was recorded. The C-fibre responses were followed for one hour after administration.

3.1.6 Statistics

In the gene expression study, the fold expression of the target genes was normalized to β-actin and the native group. The fold expression of CD68 was normalized to β-actin. Samples with a β-actin expression ≤0.01 ng were excluded from further analysis. Group means were compared using One-Way Analysis of Variance (ANOVA) with Tukey post-hoc test. A linear regression analysis was performed to study the correlation between IFN-γ and CD68.

In the electrophysiological experiments, baseline (six stimuli) and post-baseline (15 stimuli) responses were recorded. Three and three consecutive responses were converted to an average before analyzed, which produced two baseline and five post-baseline points, respectively. The C-fibre responses during one hour were analyzed with repeated measure ANOVA. At the end point, reflecting the three last responses (corresponding to the last post-baseline value), means were compared using One-Way ANOVA with Tukey post-hoc test.

SPSS version 21 was used to perform the statistical analysis. A *p*-value less than 0.05 were set as a level of statistical significance. All data are givens as mean ± standard error of the mean (SEM).

3.2 The clinical study

3.2.1 Subjects

As previously described (Olsen *et al.* 2012) all patients were recruited from Oslo University Hospital (OUS), Ullevål, Norway and Haukeland University Hospital (HUS), Norway in the period of 2007-2009. Only patients with lumbar radicular pain were considered for inclusion. The inclusion criteria were age between 18 and 60 years, lumbar disc herniation confirmed by magnetic resonance imaging (MRI) with sciatic pain and positive straight leg raising test. The exclusion criteria included lumbar spinal stenosis, previous surgery for herniated disc at the same level or fusion at any level in the lumbar spine, generalized musculoskeletal pain, inflammatory rheumatic disease, diabetic polyneuropathy, cardiovascular disease, cancer, psychiatric disease, neuronal disease, alcohol or drug abuse, completion of another surgery within one month, pregnancy, non-detectable genotype, non-European Caucasian ethnicity or poor Norwegian language.

A total of 258 patients were included in the study. 6 patients changed their minds and did not proceed, which gave us data from 252 patients.

All participants received written information and signed an informed consent form. The study was approved by the Norwegian Social Science Data Service and by the Norwegian Regional Committee for Medical Research Ethics.

3.2.2 Clinical procedure

The patients were referred from their local general practitioner (GP) to either OUS or HUS. At time of inclusion, the pain and disability was measured before treatment. For treatment timeline see figure 3.7.

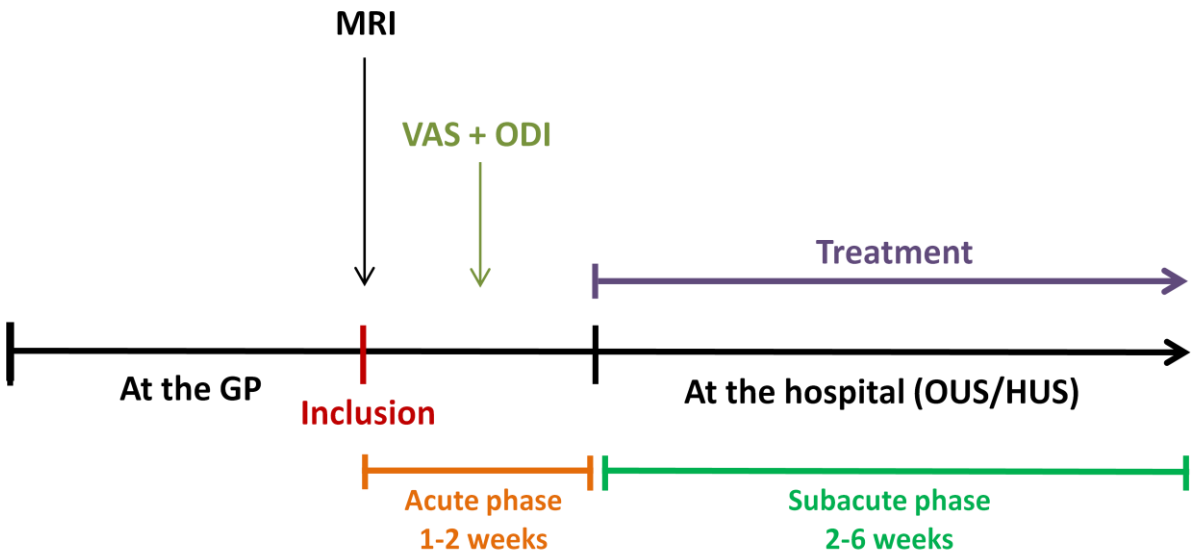

Figure 3.7: Timeline for patient treatment. The patients were first examined by their GP, before referred to either OUS or HUS. At the time of inclusion an MRI scan was performed to confirm disc herniation. Pain intensity and disability in the acute phase was measured. GP: General Practitioner; HUS: Haukeland University Hospital; MRI: Magnetic Resonance Imaging; ODI: Oswestry Disability Index; OUS: Oslo University Hospital; VAS: Visual Analogue Scale.

All the clinical data were sampled before the genotyping of the patients started.

3.2.3 Clinical measures

To measure the pain, all patients were asked to rate their pain intensity in activity during the last week on a 10-cm visual analogue scale (VAS) with endpoints “no pain” and “worst possible pain”. The validated Norwegian version of the oswestry disability index (ODI) (Grotle *et al.* 2003) was used to measure the sensory components of the pain experience and to assess problems with physical function related to low back pain.

3.2.4 DNA extraction

Blood samples were taken from the patients and the genomic DNA was extracted from whole blood cells using FlexiGene DNA isolation kit (Qiagene, Hilsen, Germany). The DNA was quantified by measuring optical density on a spectrophotometer (Eppendorf AG, Hamburg, Germany). The DNA samples were diluted in TE-buffer to achieve an approximate concentration of 20 ng/µl. For protocol see appendix 6.

3.2.5 SNP genotyping

Genotyping assays (Applied Biosystems, Foster City, CA, USA) with predesigned TaqMan SNPs for IFN-γ rs2069705, rs1861494 and rs2069718 were used to perform the TaqMan genotyping. 10 ng genomic DNA was mixed with TaqMan genotyping mastermix (Applied Biosystems, USA) and assay mix (containing primers and probes) in a 5 µl reaction mixture and amplified. The probes in the assay mix were labeled with reporter dyes, either FAM or VIC, at the 5' end to distinguish between the two alleles. A non-fluorescent quencher dye was attached to the 3' end of the probes. The reaction was performed on an ABI 7900HT sequence detector system (Applied biosystems, USA) on the following program: 10 minutes initial denaturation and enzyme activation at 95°C followed by 40 cycles at 95°C for 15 seconds and 60°C for 1 minute. Non-template controls (NTC), with water instead of DNA, were included in every run. Genotypes were determined using the SDS 2.2 software (Applied Biosystems). 10 % of the genotyped samples were run twice to ensure a reproducible result. For protocol see appendix 7. The TaqMan principle is illustrated in figure 3.8.

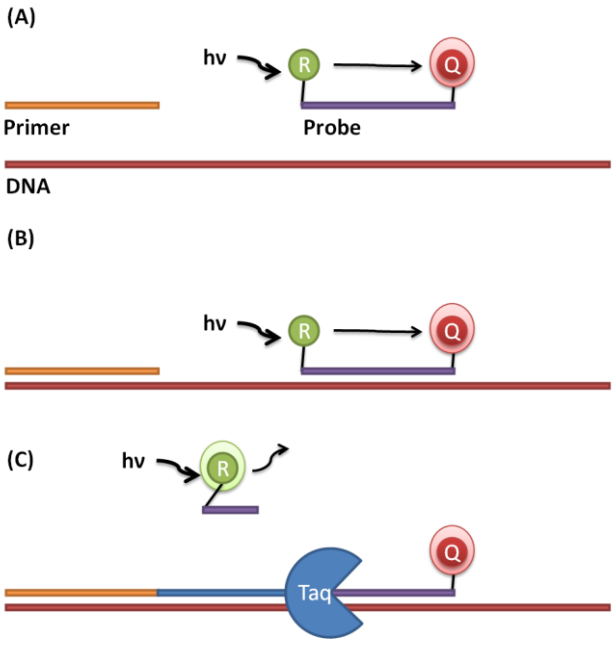

Figure 3.8: The principle of the TaqMan method. Depending on the genotype of the patients, either the VIC or FAM probe hybridizes to the DNA in the region where the SNP is present. The Taq Polymerase uses its 5' exonuclease activity to cleave the probe hybridized to the target sequence. Increase in fluorescence takes place when the reporter is cleaved from the quencher, indicating a genotype. A) The primer and probe used in TaqMan before annealing. The quencher inhibits any fluorescence signals from the reporter. B) The primer and probe anneals with the single stranded DNA molecule. C) Taq Polymerase synthesizes a new DNA strand (5'→3') from the primer and breaks the probe. The fluorescence signal from the reporter can be detected. hv: light; Q: Quencher; R: Reporter; Taq: Taq polymerase.

Allelic discrimination plots were made by the software on the basis of the fluorescence intensities of the two allele specific probes in each sample. A representative plot can be viewed in figure 3.9.

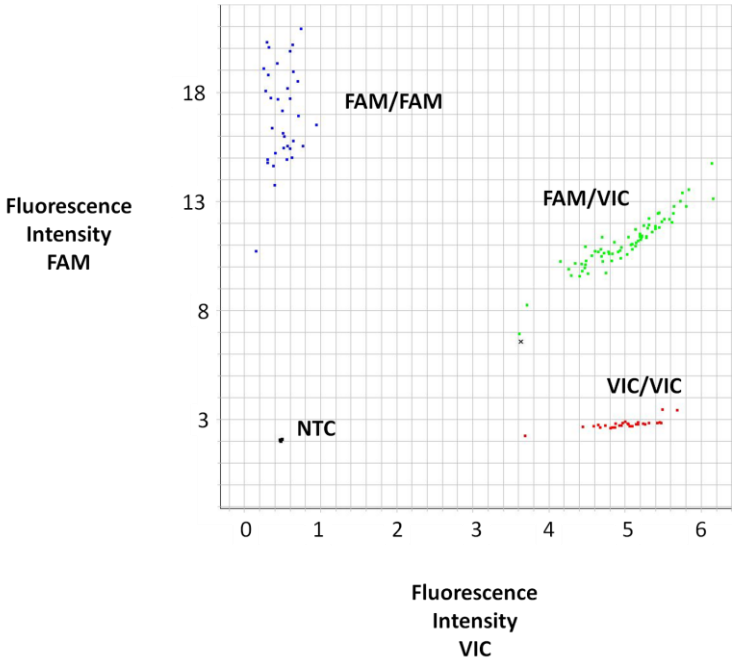

Figure 3.9: Allelic Discrimination plot from a representative genotyping run. One dot illustrates one patient's genotype. Blue indicates a FAM/FAM (homozygote) genotype. Green indicates a FAM/VIC (heterozygote) genotype. Red indicates a VIC/VIC (homozygote) genotype. The x indicates a patient who was not genotyped in this run. Black is non-template controls. NTC: Non-template control.

3.2.6 Statistics

In the clinical study VAS activity and ODI scores were analyzed regarding genotype. Group means were compared using One-Way ANOVA with Tukey post-hoc test.

SPSS version 21 was used to perform the statistical analysis. A *p*-value less than 0.05 were set as a level of statistical significance. All data are givens as mean ± SEM.

4 Results

4.1 The animal study

4.1.1 Investigation of change in gene expression in NP tissue

A PCR screening from two pooled cDNA samples (exposed vs. native) was performed to investigate the change in gene expression. It appeared to be a change in fold expression of many genes in NP tissues exposed to the dorsal nerve roots (table 4.1). The data indicated that 22 of 84 genes showed >4-fold up-regulation. The genes were ranked on relative fold expression (table 4.2). Il-1β, a cytokine earlier demonstrated to be significantly up-regulated in NP exposed for the dorsal nerve roots, was used as a positive control.

Table 4.1: The result from the screening of Rat Common Cytokine RT-PCR array

	1	2	3	4	5	6	7	8	9	10	11	12
A	Adipoq 3,18	Aimp1 -1,04	Areg 4,58	BMP-1 1,17	BMP-2 4,22	BMP-3 2,83	BMP-4 3,58	BMP-5 5,14	BMP-6 -1,16	BMP-7 4,58	C5 2,28	CD40lg 3,33
B	CD70 5,9	CNTF 1,06	CSF-1 1,89	CSF-2 3,83	CSF-3 4,03	Ctf1 1,3	FASlg 2,12	FGF-10 2,82	GDF-15 3,49	GDF-5 3,18	GDF-9 6,04	Grem1 -4,36
C	IFN-a1 3,75	IFN-a2 4,18	IFN-a4 4,53	IFN-1b 7,42	IFN-g 4,58	IL-10 2,49	IL-11 5,9	IL-12a 2,56	IL-12b 3,84	IL-13 3,58	IL-15 1,47	IL-16 2,16
D	IL-17a 2,91	IL-17b 3,27	IL-17f 2,47	IL-18 1,16	IL-1a 1,08	IL-1b 5,34	IL-1rn 3,27	IL-2 1,91	IL-20 4,47	IL-21 3,97	IL-22 3,58	IL-23a 1,47
E	IL-24 3,35	IL-27 3,93	IL-3 2,62	IL-33 3,53	IL-4 4,29	IL-5 5,16	IL-6 3,09	IL-7 1,40	IL-9 3,46	Inha 2,29	Inhab 2,89	LIF 2,96
F	Lta 2,37	Ltb 4,12	MIF 1,68	Mstn 5,71	Nampt 1,02	Nodal 4,16	Nrg1 2,30	Osm 4,78	Scgb3a1 4,39	Spp1 -1,13	TGF-b1 -1,03	TGF-b2 -1,27
G	Thpo 1,30	TNF 4,39	TNFRsf11b 2,65	TNFRsf10 3,08	TNFRsf11 2,64	TNFRsf12 1,63	TNFRsf13 2,65	TNFRsf15 1,26	TNFRsf18 2,59	TNFRsf4 2,21	TNFRsf9 3,94	VEGFa -1,33
H	b-Act	B2m	Hprt1	Ldha	Rplp1	RGDC	RTC	RTC	RTC	PPC	PPC	PPC

Fold > 5 | Fold 4-5 | Fold < 4 | = Housekeeping genes and controls

The table shows the changes in gene expression between the NP tissue exposed to dorsal nerve roots for 60 minutes relative to the native NP tissue. Red indicates a fold expression change of more than a fivefold. Orange indicates a change in fold expression between four and five. Blue indicates a fold expression change lower than four. White indicates the non-cytokine controls in the array. IL-1β was used as a positive control. IL-1β: Interleukin-1β; NP: Nucleus Pulposus.

Table 4.2: Genes with >4 fold increased in gene expression from the qPCR screening

Gene of interest	Fold up-regulation	Comment
IFN-1β	7.42	Gene of interest
GDF-9	6.04	
CD70	5.90	
IL-11	5.90	
Mstn	5.71	
IL-1β	5.34	Positive control
IL-5	5.16	
BMP-5	5.14	
Osm	4.78	
Areg	4.58	
BMP-7	4.58	
IFN-γ	4.58	Gene of interest
IFN-α4	4.53	Gene of interest
IL-20	4.47	
Scgb3a1	4.39	
TNF	4.39	
IL-4	4.29	
BMP-2	4.22	
IFN-α2	4.18	Gene of interest
Nodal	4.16	
LT-β	4.12	
CSF-3	4.03	

RT-PCR Rat Common Cytokines Array, SaBiosciences (QIAGENE). Cut-off: fold change <4, Ct-value >30. IL-1β was used as a positive control. Data ranked by changes in the fold expression. Areg: Amphiregulin; BMP: Bone Morphogenic Protein; CD: Cluster of Differentiation; CSF: Colony Stimulating Factor; Ct: Cycle threshold; GDF: Growth Differentiation Factor; IFN: Interferon; IL: Interleukin; LT: Lymphotoxin; Mstn: Myostatin; Osm: Oncostatin; Scgb: Secretoglobulin; TNF: Tumor Necrosis Factor.

As IFN-1β had the highest fold changes this cytokine and the three other interferons on the list were defined as genes of interest. Hence, four genes were chosen for further qPCR investigation. Follow-up analysis of the 60 minute tissue confirmed that the up-regulation of all the four interferons were statistically significant (figure 4.1).

The observed fold change in NP tissue exposed to the spinal dorsal nerve roots relative to the native NP tissue was 11.04±2.34 for IFN-γ (p=0.016, One-Way ANOVA), 4.60±0.84 for IFN-α2 (p=0.023, One-Way ANOVA), 4.54±0.92 for IFN-1β (p=0.043, One-Way ANOVA) and 4.50±0.69 for IFN-α4 (p=0.022, One-Way ANOVA) after normalization to β-actin.

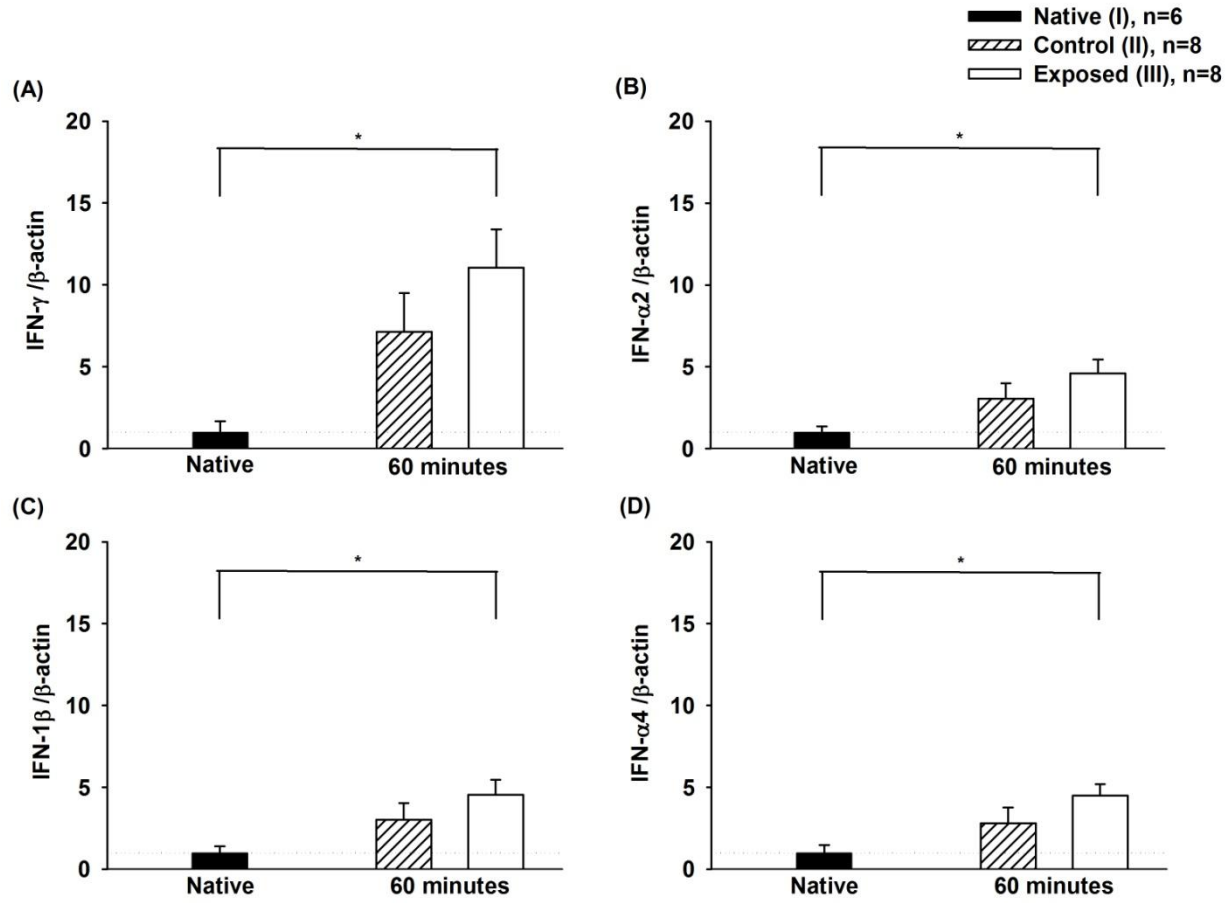

Figure 4.1: Changes in IFN gene expression in NP tissue. Gene expression of target genes relative to the reference gene β-actin in NP tissue (I) harvested from native, (II) isolated in 0.9 % NaCl for 60 minutes, or (III) exposed to the spinal dorsal nerve roots for 60 minutes. A) IFN-γ: p=0.016 (One-Way ANOVA), native vs. exposed: p=0.012 (post-hoc Tukey comparison). B) IFN-α2: p=0.023 (One-Way ANOVA), native vs. exposed: p=0.018 (post-hoc Tukey comparison). C) IFN-1β: p=0.043 (One-Way ANOVA), native vs. exposed: p=0.034, (post-hoc Tukey comparison). D) IFN-α4: p=0.022 (One-Way ANOVA), native vs. exposed: p=0.017 (post-hoc Tukey comparison). All values are normalized to the native group. *=$p \leq 0.050$. Data are given as mean ± SEM. IFN-α2: Interferon-α2; IFN-α4: Interferon-α4; IFN-γ: Interferon-γ; IFN-1β: Interferon-1β; NP: Nucleus Pulposus.

4.1.2 Macrophages in NP tissue

To investigate the possibility of macrophage activation and infiltration qPCR with CD68 and F4/80 primers were performed. A significant up-regulation of CD68 in NP tissue exposed to spinal dorsal nerve roots for 60 minutes was demonstrated (figure 4.2A). The observed up-regulation was 9.57±2.86 in the exposed group after normalization to β-actin. (p=0.042, One-Way ANOVA). Moreover, a correlation between CD68 and IFN-γ was observed (figure 4.2B-D) (Linear Regression Analysis). qPCR with F4/80 primers showed that all the C_t-values were above 30, which indicate an unreliable low concentration. The F4/80 results were therefore not analyzed.

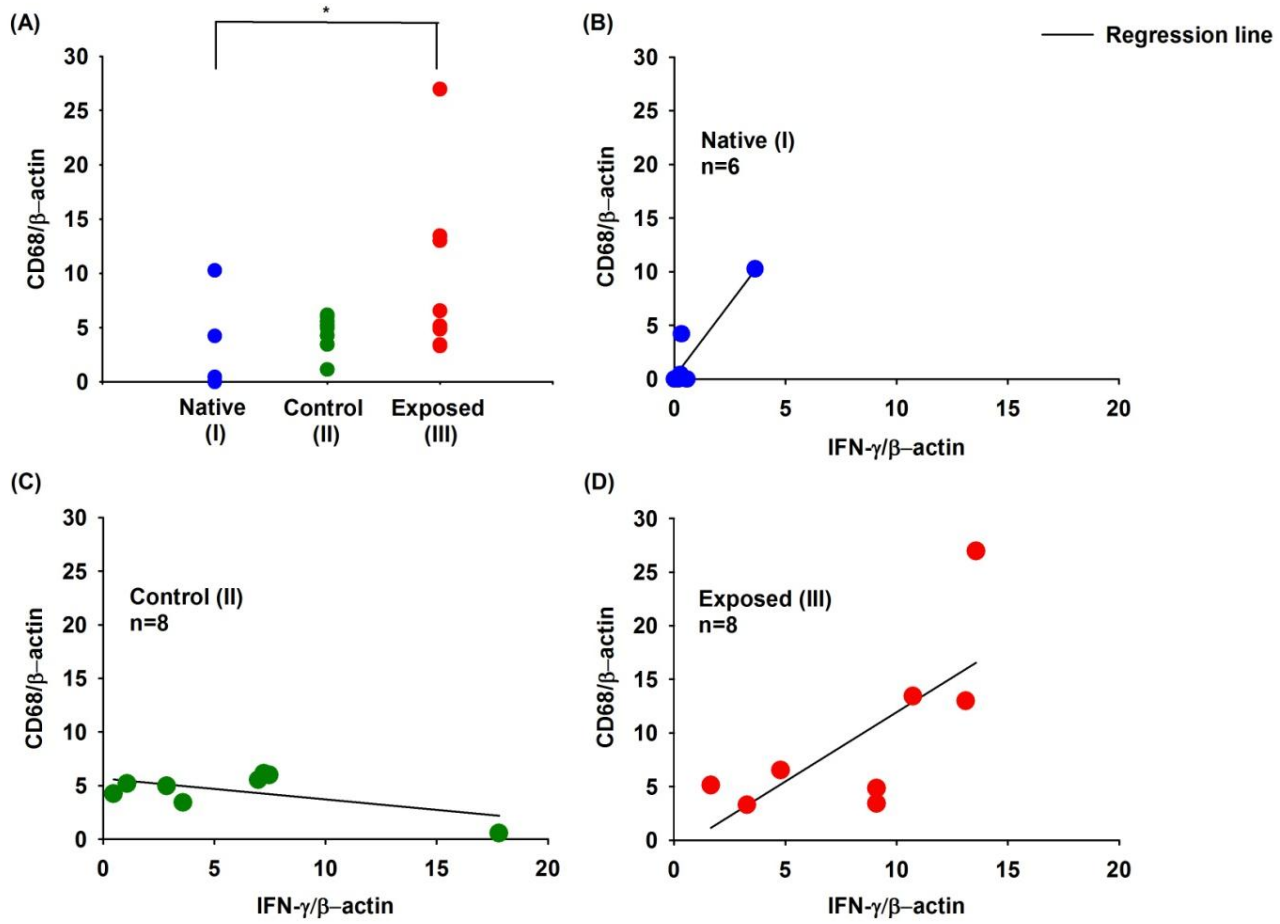

Figure 4.2: Change in CD68/IFN-γ gene expression. A) Changes in gene expression of CD68 relative to the reference gene β-actin in NP tissue (I) harvested from native, (II) isolated in 0.9 % NaCl for 60 minutes, or (III) exposed to the spinal dorsal nerve roots for 60 minutes. p=0.042 (One-Way ANOVA), native vs. exposed: p=0.043 (post hoc Tukey comparisons). B) The gene expression of CD68 vs. IFN-γ native: R^2=0.840, p=0.010 (Linear Regression Analysis). C) The gene expression of CD68 vs. IFN-γ in NP control tissue in 0.9 % NaCl for 60 minutes: R^2=0.305, p=0.156 (Linear Regression Analysis). D) The gene expression of CD68 vs. IFN-γ in NP tissue exposed to the dorsal nerve roots for 60 minutes: R^2=0.510, p=0.047 (Linear Regression Analysis). All the samples plotted together (data not shown): R^2=0.278, p=0.012 (Linear Regression Analysis). *=$p \leq 0.050$. One dot indicates the fold change for one sample. CD68: Cluster of Differentiation 68; IFN-γ: Interferon-γ; NP: Nucleus Pulposus.

4.1.3 Electrophysiological extracellular single cell recordings

Electrophysiological recordings showed a statistically significant increase in C-fibre response during one hour after application of NP and administration of IFN-γ (figure 4.3A) (p=0.000, Repeated Measure ANOVA). After 60 minutes the C-fibre responses in the NP, IFN-γ and control experiments were 127.34±7.00, 128.21±11.84 and 93.63±6.68 percent of baseline, respectively (figure 4.3B) (p=0.005, One-Way ANOVA).

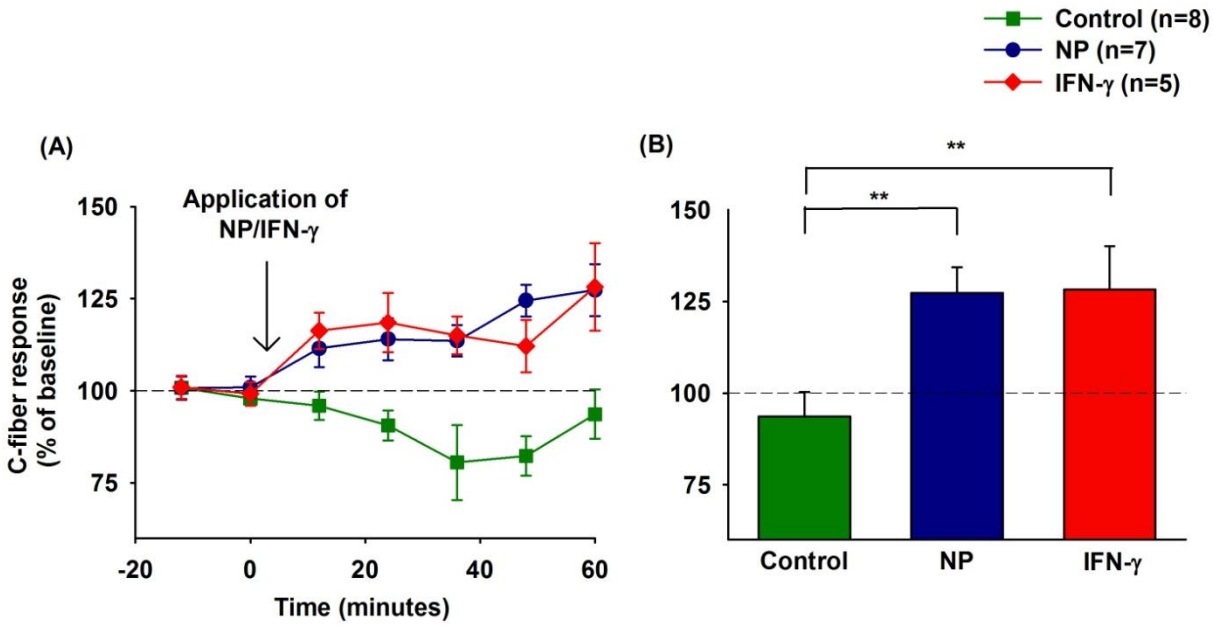

Figure 4.3: C-fibre response as a percentage of baseline. A) The electrophysiological recordings showed an increase in C-fibre response over time when NP was applied onto the spinal dorsal nerve roots compared to control experiments, as well as an increase in C-fibre response when IFN-γ was applied (p=0.000, Within-Subjects Effect, Repeated Measure ANOVA). B) At one hour there was a significant effect of NP/IFN-γ (p=0.005, One-Way ANOVA). Control vs. NP: p=0.010 (post hoc Tukey comparisons), and control vs. IFN-γ: p=0.017 (post hoc Tukey comparisons). **=$p \leq 0.010$. Data are given as mean ± SEM. IFN-γ: Interferon-γ; NP: Nucleus Pulposus.

4.2 The clinical study

Acute pain following disc herniation was measured with VAS activity and ODI scores. Patients were genotyped with regards to three IFN-γ SNPs (rs2069705 G/A, rs1861494 C/T and rs2069718 A/G). The main characteristics for the patients in the different groups can be viewed in table 4.3, 4.4 and 4.5.

The VAS activity and ODI scores for rs2069705 (figure 4.4) showed that the patients with G/G genotype had a significantly better function (i.e. lower ODI score) compared to the other two genotypes. VAS activity scores were 5.26±0.57, 6.12±0.26 and 6.55±0.22 for G/G, G/A and A/A genotype, respectively (One-Way ANOVA, p=0.063). The ODI scores were 28.34±3.36, 40.99±1.78 and 44.09±1.20 for G/G, G/A and A/A genotype, respectively (p=0.008, One-way ANOVA).

The VAS and ODI scores for rs1861494 (figure 4.5) showed that patients with C/C genotype had a significantly better function (i.e. lower ODI score) compared to the T/T genotype. The VAS activity scores were 5.34±0.69, 5.84±0.28 and 6.48±0.21 for C/C, C/T and T/T genotype, respectively (p=0.081, One-Way ANOVA). The ODI scores were 26.79±2.51, 38.70±1.85 and 40.30±1.71 for C/C, C/T and T/T genotype, respectively (p=0.030, One-Way ANOVA).

The VAS activity and ODI scores for rs2069718 (figure 4.6) demonstrated that patients with the A/A genotype showed a significantly better function (i.e. lower ODI score) compared to the A/G genotype. The VAS activity scores were 5.64±0.36, 6.21±0.25 and 6.64±0.25 for A/A, A/G and G/G genotype, respectively (p=0.095, One-Way ANOVA). The ODI scores were 33.30±2.58, 41.17±1.79 and 40.59±2.06 for A/A, A/G and G/G genotype, respectively (p=0.044, One-Way ANOVA).

Table 4.3: Characteristics of patients grouped by IFN-γ rs2069705 G/A genotypes.

	G/G n = 25	G/A n = 108	A/A n = 114
Gender, men/women (%)	13/12 (52/48)	55/53 (51/49)	63/51 (55/45)
Mean age (min-max)	39 (20-59)	42 (18-60)	44 (19-59)
Current smoker, yes/no (%)	7/18 (28/72)	41/67 (38/62)	42/72 (37/63)
Treatment, surgery/conservative (%)	9/16 (36/64)	64/44 (59/41)	71/43 (62/38)

A: Adenosine; G: Guanine.

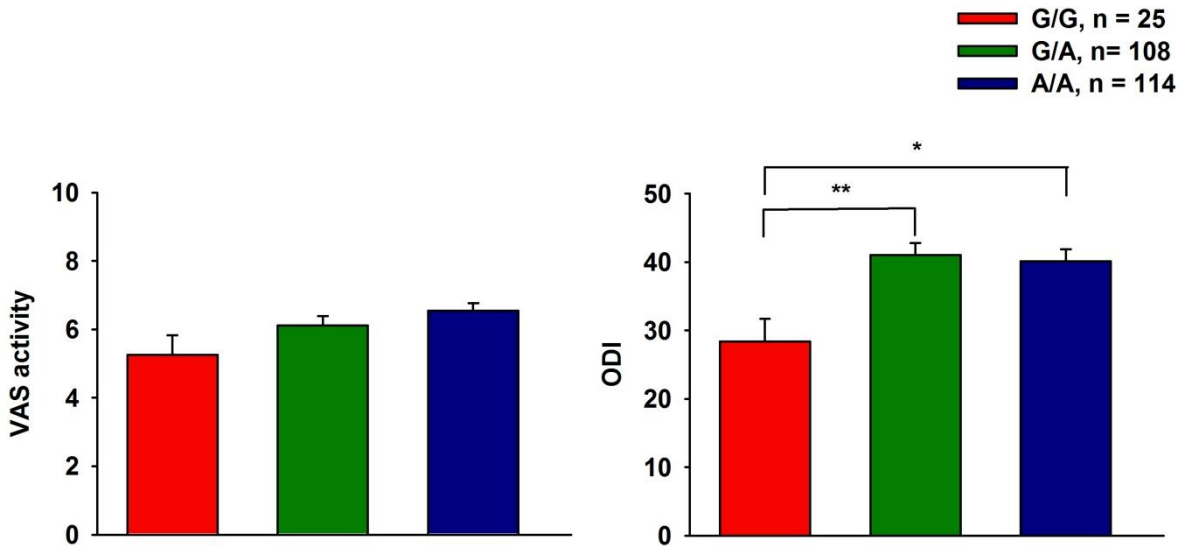

Figure 4.4: Pain and disability for IFN-γ rs2069705 G/A genotypes. VAS activity: p=0.063 (One-Way ANOVA). ODI: p=0.008 (One-Way ANOVA), G/G vs. G/A: p=0.007, G/G vs. A/A: p=0.012 (post hoc Tukey comparisons). *=$p \leq 0.05$, **=$p \leq 0.01$. Data are given as mean ± SEM. IFN-γ: Interferon-γ; ODI: Oswestry Disability Index; VAS: Visual Analogue Scale.

Table 4.4: Characteristics of patients grouped by IFN-γ rs1861494 C/T genotypes.

	C/C n = 15	C/T n = 95	T/T n = 133
Gender, men/women (%)	8/7 (53/47)	50/45 (53/47)	74/59 (56/44)
Mean age (min-max)	38 (20-59)	41 (18-60)	41 (19-59)
Current smoker, yes/no (%)	5/10 (33/67)	35/60 (37/63)	50/83 (38/62)
Treatment, surgery/conservative (%)	5/10 (33/67)	53/42 (56/44)	81/52 (61/39)

C: Cytosine; T: Tyrosine.

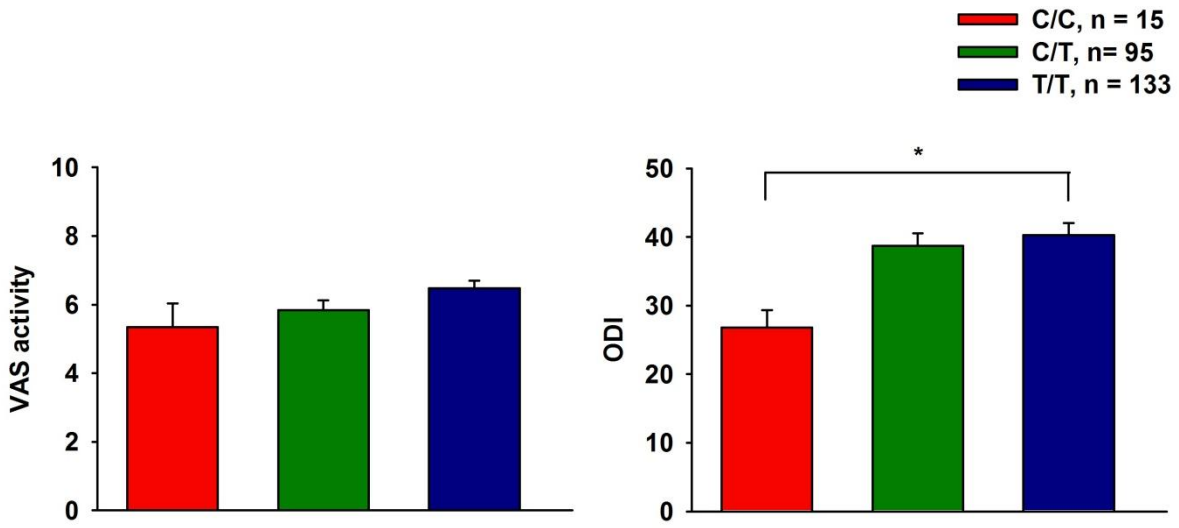

Figure 4.5: Pain and disability for IFN-γ rs1861494 C/T genotypes. VAS activity: p=0.081 (One-Way ANOVA). ODI: p=0.030 (One-Way ANOVA), C/C vs. T/T: p=0.022 (post hoc Tukey comparisons). *=$p \leq 0.05$. Data are given as mean ± SEM. IFN-γ: Interferon-γ; ODI: Oswestry Disability Index; VAS: Visual Analogue Scale.

Table 4.5: Characteristics of patients grouped by IFN-γ rs2069718 A/G genotypes.

	A/A n = 48	A/G n = 118	G/G n = 84
Gender, men/women (%)	24/24 (50/50)	62/56 (54/48)	49/37 (58/44)
Mean age (min-max)	40 (20-59)	42 (18-60)	41 (19-59)
Current smoker, yes/no (%)	16/32 (33/67)	46/72 (39/61)	30/54 (36/65)
Treatment, surgery/conservative (%)	23/25 (48/52)	67/51 (57/43)	56/28 (67/33)

A: Adenosine; G: Guanine.

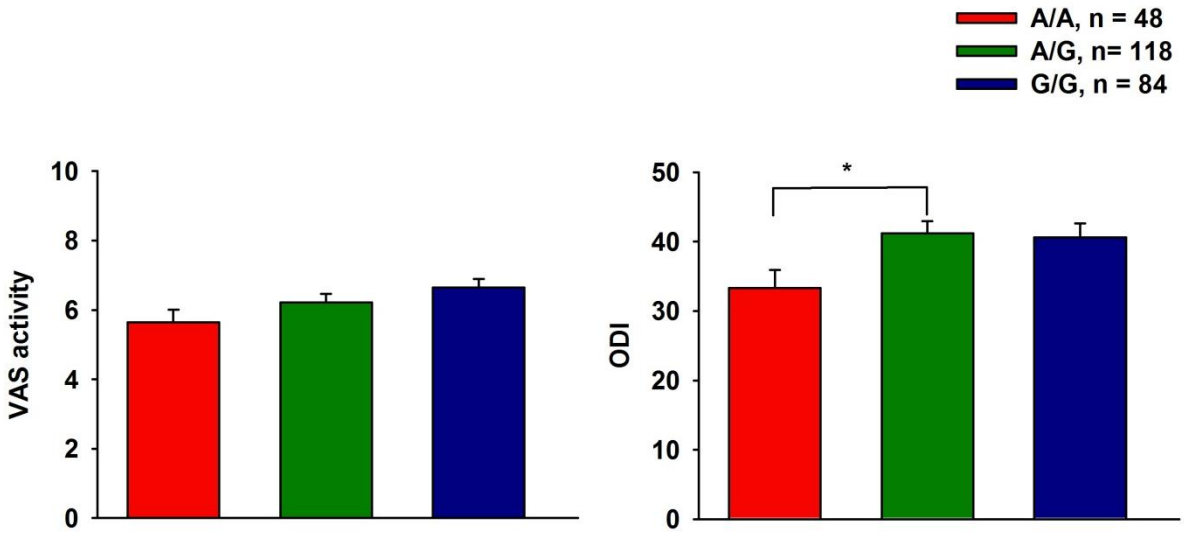

Figure 4.6: Pain and disability for IFN-γ rs2069718 A/G genotypes. VAS activity: p=0.095 (One-Way ANOVA). ODI: p=0.044 (One-Way ANOVA), A/A vs. A/G: p=0.042 (post hoc Tukey comparisons). *=$p \leq 0.05$. Data are given as mean ± SEM. IFN-γ: Interferon-γ; ODI: Oswestry Disability Index; VAS: Visual Analogue Scale.

5 Discussion of methods

5.1 The animal study

Lewis rats have a more pronounced inflammatory response to injury compared to other rats, such as Sprague-Dawley (Popovich *et al.* 1997) used in previous experiments (Pedersen and Gjerstad 2008; Jacobsen *et al.* 2010). Our goal was to the study inflammatory processes close to the dorsal nerve roots, and Lewis rats were therefore chosen in this present study.

Working with male rats can lead to increased risk of allergy in laboratory workers (Renstrom *et al.* 2001), and female rats were therefore preferred. Previous studies suggest that the pain threshold can vary with the estrous cycle in female rats, with a pain sensitivity peak during late proestrus and early estrus phase. For review see (Fillingim and Ness 2000). However, in our lab, all the experiments were done in a randomized order. Individual differences in the estrous cycle were therefore not assumed to interfere with the outcome of the different groups.

Urethane (ethyl carbamate) is often used as an anesthetic for animal studies because of its long-lasting surgical anesthesia. However, because of carcinogenic properties it is not used in clinical settings, or in animal survival surgery. In our study, urethane was used because of its minimal effect on many systems including the cardiovascular- (Maggi and Meli 1986b) and the neuronal system (Maggi and Meli 1986a). Anesthetics can influence neurotransmitter-gated ion channels, but earlier data indicate only a weak effect of urethane on ion channels such as AMPA and NMDA compared to other anesthetics (Hara and Harris 2002). The urethane dose used in the present experiments (1.8-2.7 mg/kg bodyweight) is in agreement with previous studies (Gjerstad *et al.* 2005; Pedersen *et al.* 2010; Egeland *et al.* 2013).

5.1.1 Gene expression analysis

To mimic the clinical situation after disc herniation NP tissue, from genetic identical donor rats, was applied onto the spinal dorsal nerve roots. In previous studies NP tissue have been harvested from the same animal used in the experiment (Anzai *et al.* 2002; Cuellar *et al.* 2005). However, trauma from NP harvesting can be avoided by using donor rats (Kallakuri *et al.* 2005). In addition it would have been difficult to access NP during electrophysiological recording, as will be described later.

RNA is fragile and very easy to degenerate or contaminate outside its normal environment. To make sure that the RNA was of good quality, an Agilent Bioanalyzer was used to measure the RIN-values. A RIN-value indicates the degree of RNA degeneration in a sample. It is important to have intact RNA before cDNA synthesis to ensure a reproducible and reliable result. The RIN-values also give a standardized measure of RNA quality, which ensures reproducible results across different labs (Imbeaud *et al.* 2005).

There are several ways to quantify mRNA, such as northern blotting, in situ hybridization, RNase protection assays and qPCR. However, qPCR is the only highly sensitive method. In addition qPCR make it possible to discriminate between very similar mRNAs. This is an advantage when the goal is to quantify gene expression from relatively small NP tissue samples, as well as discriminate between genes closely related. For review see (Bustin 2000).

SYRB Green is, as previously described, an intercalating dye that binds to any amplified DNA. It is therefore very important to analyze the qPCR results carefully to obtain the right results. Melting curves with more than one peak, indicating more than one PCR product, were used as an exclusion criterion. Primers were designed to span introns, to avoid amplification of genomic DNA. BLAST searches were also performed to make sure that the primer sequences were specific for the target gene. Only primers with GC content of 30-70 % (if possible 40-60 %), a length of 18-30 bp and a melting temperature (T_m) between 55-60°C were used. In addition T_m should not vary more than 1-2°C within one primer pair. All included primers and qPCR runs fit these criteria.

To correct for sample to sample variations, such as differences in the amount of starting tissue or different cDNA synthesis efficiency, all target gene expressions were normalized to the reference gene β-actin. All samples were also run in parallel and the mean value were used to minimize human error. In cases where the two parallels had large differences, the parallel with the seemingly most correct amplification plot was used to determine the quantity.

Samples with β-actin values under 0.01 ng were excluded. A C_t-value over 30 was also set as a cutoff to make sure that unreliably low concentration of the target gene was not included. F4/80 was therefore not analyzed.

The interferons were normalized to the native samples, so that relative gene expression could, without PCR run differences, be compared to each other. The fold expression in the control tissue and tissue exposed to the dorsal nerve roots was not normalized to the native group for

CD68. Normalization to the native group would have given CD68 an unreliable fold change since CD68 was absent in four out of six native samples. IFN-γ, used in the regression analysis with CD68, was therefore not normalized to native only to β-actin.

In general mRNA is translated to proteins, and the change in fold expression therefore suggests a change in protein concentration. However, we have not measured the actual increase in protein concentration and can therefore not be sure that the mRNA is actually translated into functional protein.

5.1.2 Electrophysiological extracellular single cell recordings

Several electrophysiological techniques can be used to study neuronal activity, including nociceptive signaling from the dorsal horn. In-vitro whole cell patch-clamp recordings of lamina I neurons in slices (Ikeda *et al.* 2003) is one example. These types of studies allow controlling of the cellular environment. It is also easier to maintain a stable recording over a long period of time, without interference of anesthetics. However, in slices the neuronal activity is studied without the influence of circulating mediators and descending pathways. Cell recordings in an in-vivo system, in contrast, give us the possibility to study complex physiological responses. This technique was preferred in the present experiments.

The neuronal activity in the dorsal horn have previously been measured using extracellular in-vivo techniques such as field potential recordings (Hjornevik *et al.* 2010; Jacobsen *et al.* 2010) and single unit recordings (Pedersen *et al.* 2010; Egeland *et al.* 2013). Both techniques make it possible to observe the changes in C-fibre response, which are thought to be important for the development of chronic pain. However, it is easier to quantify the change in C-fibre response using single cell recording. The technique was therefore used in the present study.

To get accurate results it is important to ensure that recordings throughout the experiments are only performed on one cell. Amplitude and shape were therefore carefully analyzed. However, it is not possible to be absolutely certain that only one cell is studied as some cells may have similar amplitude and shape (Miki *et al.* 2002). Some recording bias can therefore occur.

NP application and IFN-γ administration

Recent data demonstrate that NP applied onto the spinal dorsal nerve roots may enhance the C-fibre response in the dorsal horn (Egeland *et al.* 2013). In contrast, adipose tissue has not been shown to change the neuronal firing (Aoki *et al.* 2002; Brisby and Hammar 2007), indicating that mechanical pressure does not affect the C-fibre response. Moreover, there is no evidence that adipose tissue have any other effect on neuronal tissue than saline control (Cuellar *et al.* 2004). A saline control was therefore chosen in this study.

When performing single cell recordings in the dorsal horn it is best to avoid disturbances to the animal. The experimental set-up did not give good access to harvest NP during recording, and NP was therefore harvested from a donor rat using the same procedure as in the gene expression study.

To study the effect of IFN-γ, a recombinant rat protein was used. After a stabile baseline, 1000 U was administrated directly onto the spinal cord in one dose. By administrating the protein directly onto the dorsal nerve roots and spinal cord IFN-γ could bind to receptors on the spinal dorsal nerve roots and in the dorsal horn. IFN-γ in this dose has previously been described to activate microglia and induce tactile allodynia in rats (Tsuda *et al.* 2009), as well as induce an increased excitability and loss of inhibition in the dorsal horn (Vikman *et al.* 2005).

5.2 The clinical study

5.2.1 Patients

The patients were recruited from OUS and HUS. Only patients with lumbar radicular pain and disc herniation confirmed with MRI were considered for inclusion in the study. The strict inclusion and exclusion criteria were as previously described (Olsen *et al.* 2012). As genetic variation between different ethnicities occur more frequently than within one ethnic population, all non-European Caucasian were excluded from the genetic analysis. Thus the genetic variation within the patient population was decreased.

The study consisted of 252 patients between 18 and 60 years of age, with an approximately even distribution between the sexes. One limitation with the analyzed material is that no co-

factors have been corrected for. In addition, the patients received different medications before inclusion when VAS and ODI was recorded.

5.2.2 VAS and ODI

VAS has previously been validated to score pain (Crossley *et al.* 2004; Boonstra *et al.* 2008), and ODI is a validated questionnaire to measure disability outcome after spinal trauma (Fairbank and Pynsent 2000). With ODI physical activity, not psychological consequences of acute or chronic pain, is reported. Pain intensity, personal care, lifting, walking, sitting, standing, sleeping, sex life, social life and travelling is measured, and in each category the patients will select one of six statements, giving a score of zero to five. A higher score indicates a higher disability.

5.2.3 Genotyping

Genotyping is prone to errors and it has been suggested that an error rate of 0.5-1.0 % can alter medical relevant results (Abecasis *et al.* 2001). Problems with DNA quality or quantity, errors with the DNA sequence (such as mutations near the SNP), biochemical artifacts (such as errors with the equipment or with Taq polymerase) or human error may cause genotyping errors.

In the present study predesigned IFN-γ TaqMan SNP genotyping assays were used. To avoid human genotyping errors, the software performed all allelic discriminations, as done in previous studies (Jacobsen *et al.* 2012; Olsen *et al.* 2012). DNA samples with poor quality, resulting in an un-detectable genotype, were excluded from further analysis. To ensure that the genotyping results were reliable, 10 % were tested twice, always giving the same result. Non-template controls were also included in every run.

6 Discussion of results

6.1 The animal study

NP has previously been described to increase the excitability of the dorsal horn neurons when applied onto the spinal dorsal nerve roots (Egeland *et al.* 2013). In the present study we demonstrate an increase in C-fibre response to test stimuli during one hour after NP application, compared to control experiments. A clear increase in the C-fibre response was seen already 12 minutes after application of NP tissue. This rapid effect suggests that NP tissue may have a direct effect on neuronal tissue through ion channels.

Other studies have also shown a pro-nociceptive effect of NP tissue. Application of NP onto DRG has been shown to increase thalamic responses (Brisby and Hammar 2007), enhance responses of WDR neurons to noxious stimuli (Anzai *et al.* 2002) and enhance wind-up in the dorsal horn (Cuellar *et al.* 2005). An increase in mechanical hypersensibility and increased excitability has also been demonstrated when NP is applied onto the dorsal nerve roots (Takebayashi *et al.* 2001). In addition, behavioral studies show that NP applied onto the DRG may cause pain (Olmarker 2008). These previous findings suggest that NP has important effects on the dorsal horn neurons and the nociceptive pathways.

Non-mechanical effects after disc herniation are thought to be associated with cytokines release from intervertebral disc cells (Olmarker *et al.* 1993; Rothwell and Strijbos 1995). IFN-γ has been suggested to be involved because of its neurotoxic properties (Hartung *et al.* 1992). Studies comparing disc injury without NP leakage vs. NP exposure and no disc injury have demonstrated that pain behavior is a response to NP tissue coming in contact with neuronal tissue, not the disc injury itself. (Nilsson *et al.* 2011).

In the present study we demonstrated an up-regulation of IFN-γ, IFN-α2, IFN-1β and IFN-α4 in NP tissue after application onto the dorsal nerve roots. We also found an up-regulation of CD68, a known marker of macrophage activation, in the same tissue. No detectable expression of F4/80, a marker specific for macrophages from the myeloid lineage, was demonstrated.

CD68 has previously been used to demonstrate infiltration of circulating macrophages into NP tissue (Kawaguchi *et al.* 2001). However, because of the lack of blood supply to NP it is

unlikely that bone marrow-derived macrophages are present in the intact disc. Moreover, phagocytic CD68+ cells in degenerative NP have been reported. These phagocytic CD68+ cells are morphologically similar to other NP cells under the microscope, further establishing tissue-specific macrophages as a part of NP tissue (Nerlich *et al.* 2002).

IFN-γ can activate macrophages. It is therefore reasonable to assume that tissue specific macrophages within NP are activated upon disc herniation. Activated macrophages will produce and release IFN-γ. This serves as a self-propagating feed-back reaction, which increases the IFN-γ production and further activates more phagocytic cells. A significant relationship between IFN-γ and CD68 in NP tissue exposed to the dorsal nerve roots was also observed. Our data therefore suggest that IFN-γ activates tissue-specific macrophages and that the increase in fold expression of CD68 is not related to macrophage infiltration, but activation of already existing phagocytic cells within the NP tissue.

Our data did not show any clear differences in gene expression between NP tissue in contact with the dorsal nerve roots vs. the saline control. This suggests that the mechanical trauma of tissue harvesting, together with the change in milieu, may be enough to activate tissue-specific macrophages. It is tempting to speculate that an unknown co-factor in the spinal cord is crucial for a large scale activation of the NP macrophages, and thereby a significant up-regulation of the IFNs.

IFN-γ was the most up-regulated cytokine in NP tissue exposed for the spinal dorsal nerve roots after one hour. To investigate if the cytokine could mimic the neuronal excitable effect of NP it was applied onto the dorsal nerve roots, and the C-fibre response was recorded. At the one hour time point there were no differences between the IFN-γ recordings and the recordings with NP tissue. On the other hand, both data sets were different from the control experiments. These results indicate a functional effect of IFN-γ on the spinal dorsal nerve roots, similar to the effect of NP.

IFN-γ has been linked to an increase in spontaneous excitatory activity in dorsal horn neurons and thereby induce characteristics of central sensitization (Vikman *et al.* 2003). IFN-γ is also suggested to induce neuronal dysfunction trough an IFN-γ receptor-GluR1 complex (Mizuno *et al.* 2008), leading to neuropathic pain-related behavior in animal studies (Robertson *et al.* 1997).

The AMPA receptor subunit GluR1 can almost exclusively be found on inhibitory interneurons (Kerr *et al.* 1998). The IFN-γ receptor may form a calcium-permeable receptor complex with GluR1 after phosphorylation via the JAK1-2/STAT1 pathway. The effect of IFN-γ is therefore an increase in Ca^{2+} influx, followed by an increase in NO concentration and decrease in ATP production (Mizuno *et al.* 2008). This cascade can lead to a neuronal dysfunction of the inhibitory interneurons, which again can induce characteristics of central sensitization.

It is likely that IFN-γ, secreted from the tissue-specific macrophages in NP, may affect neurons in the dorsal horn important for nociceptive signaling. We therefore suggest that IFN-γ may be an important cytokine in the acute pain phase following disc herniation, leading to a reduced activity in the spinal inhibitory interneurons and subsequent central sensitization. In patients this can contribute to persistent pain after disc herniation.

6.2 The clinical study

To follow-up the result from the animal research, three IFN-γ SNPs were tested on 252 patients in the acute phase following disc herniation. A trend was observed in the VAS activity scores, illustrating that the genotypes may have an effect on pain. We further demonstrate a significant contribution of the three IFN-γ SNPs in regards to disability measured by ODI. The present findings may suggest an important role for IFN-γ in the early stages of inflammation after disc herniation.

As previously described rs2069705 is a promoter SNP reported to be associated with transcription rate and expression level of IFN-γ (Kim *et al.* 2010). The present study supports these previous findings. Moreover, our data suggest that the A/A and A/G genotypes are associated with a higher expression of IFN-γ and thereby more pronounced symptoms after disc herniation.

Previous studies have also suggested that the T allele for the intron 3 rs1861494 SNP have a higher binding affinity for nuclear factors than the C allele (Kumar and Ghosh 2008). This is supported by our finding, which demonstrates a significantly lower function and thereby higher disability for patients with T/T genotype.

The intron 3 SNP rs2069718 is also thought to influence the gene expression of IFN-γ (Kim *et al.* 2010). Our present findings suggest the A/A genotype is associated with a lower expression of IFN-γ, correlating with better function and lower disability following disc herniation.

Taken together, these results indicate that genetic variations can lead to an increase in expression of IFN-γ, thus may be important for the inflammatory process close to the dorsal nerve roots in the acute phase following disc herniation.

7 Conclusion

I. An up-regulation of four interferons in NP tissue one hour after application onto the spinal dorsal nerve roots was observed. IFN-γ, a neurotoxin, known to activate both macrophages and microglia, was most up-regulated. These findings indicate that NP tissue in contact with the spinal dorsal nerve roots may have neurotoxic effect, as well as activate immune cells.

II. The NP tissue exposed to the dorsal nerve roots for one hour showed an up-regulation of CD68, a marker for lysosomal activity and macrophage activation. In contrast no detectible amount of F4/80, a marker for blood-borne macrophages, was found. This suggests that activation of tissue-specific macrophages may be important in inflammation following disc herniation.

III. NP tissue applied onto the spinal dorsal nerve roots increased the excitability of the dorsal horn neurons. Already after 12 minutes a clear increase in the number of C-fibre spikes was observed, suggesting that NP may influence ion channels in the acute phase following disc herniation.

IV. Administration of IFN-γ onto the spinal dorsal nerve roots increased the excitability of dorsal horn neurons in the same way as NP tissue. The C-fibre response continued to increase during the experiment, as observed after application of the NP tissue. Previous data have shown that IFN-γ may influence the AMPA receptor on inhibitory interneurons and lead to disinhibition and subsequent sensitization. Hence, our data indicates that NP up-regulation of IFN-γ may be followed by nerve dysfunction and central sensitization following disc herniation.

V. Finally, it was demonstrated that three SNPs (rs2069705, rs1861494 and rs2069718) in the IFN-γ gene may be associated with disability in the acute phase following disc herniation in 252 sciatica patients. This suggests that these three SNPs may be important for regulation of transcription rate and thereby IFN-γ concentration in and around the herniated disc.

In summary, the increase in fold expression of IFN-γ may be a result of activation of tissue-specific macrophages in NP. IFN-γ may increase the neuronal excitability of the pain pathways. Taken together, our data suggest that IFN-γ may be important for the pathogenesis, pain experience and disability in acute lumbar radicular pain following disc herniation.

References

Abecasis, G. R., et al. (2001). "The impact of genotyping error on family-based analysis of quantitative traits." Eur J Hum Genet **9**(2): 130-134.

Anzai, H., et al. (2002). "Epidural application of nucleus pulposus enhances nociresponses of rat dorsal horn neurons." Spine (Phila Pa 1976) **27**(3): E50-55.

Aoki, Y., et al. (2002). "Local application of disc-related cytokines on spinal nerve roots." Spine (Phila Pa 1976) **27**(15): 1614-1617.

Basbaum, A. I., et al. (2009). "Cellular and molecular mechanisms of pain." Cell **139**(2): 267-284.

Boonstra, A. M., et al. (2008). "Reliability and validity of the visual analogue scale for disability in patients with chronic musculoskeletal pain." Int J Rehabil Res **31**(2): 165-169.

Brisby, H. and I. Hammar (2007). "Thalamic activation in a disc herniation model." Spine (Phila Pa 1976) **32**(25): 2846-2852.

Brookes, A. J. (1999). "The essence of SNPs." Gene **234**(2): 177-186.

Buckwalter, J. A. (1995). "Aging and degeneration of the human intervertebral disc." Spine (Phila Pa 1976) **20**(11): 1307-1314.

Bustin, S. A. (2000). "Absolute quantification of mRNA using real-time reverse transcription polymerase chain reaction assays." J Mol Endocrinol **25**(2): 169-193.

Calabrese, V., et al. (2007). "Nitric oxide in the central nervous system: neuroprotection versus neurotoxicity." Nat Rev Neurosci **8**(10): 766-775.

Carvalho, A. L., et al. (2000). "Regulation of AMPA receptors by phosphorylation." Neurochem Res **25**(9-10): 1245-1255.

Cervero, F. (1995). "Visceral pain: mechanisms of peripheral and central sensitization." Ann Med **27**(2): 235-239.

Chen, B. S. and K. W. Roche (2007). "Regulation of NMDA receptors by phosphorylation." Neuropharmacology **53**(3): 362-368.

Chen, Y. F., et al. (2013). "Insights into the hallmarks of human nucleus pulposus cells with particular reference to cell viability, phagocytic potential and long process formation." Int J Med Sci **10**(13): 1805-1816.

Cohn, Z. A., et al. (1966). "The in vitro differentiation of mononuclear phagocytes. V. The formation of macrophage lysosomes." J Exp Med **123**(4): 757-766.

Crossley, K. M., et al. (2004). "Analysis of outcome measures for persons with patellofemoral pain: which are reliable and valid?" Arch Phys Med Rehabil **85**(5): 815-822.

Cuellar, J. M., et al. (2013). "Cytokine expression in the epidural space: a model of noncompressive disc herniation-induced inflammation." Spine (Phila Pa 1976) **38**(1): 17-23.

Cuellar, J. M., et al. (2005). "Application of nucleus pulposus to L5 dorsal root ganglion in rats enhances nociceptive dorsal horn neuronal windup." J Neurophysiol **94**(1): 35-48.

Cuellar, J. M., et al. (2004). "Role of TNF-alpha in sensitization of nociceptive dorsal horn neurons induced by application of nucleus pulposus to L5 dorsal root ganglion in rats." Pain **110**(3): 578-587.

DeLeo, J. A., et al. (1996). "Interleukin-6-mediated hyperalgesia/allodynia and increased spinal IL-6 expression in a rat mononeuropathy model." J Interferon Cytokine Res **16**(9): 695-700.

Dinarello, C. A. (2000). "Proinflammatory cytokines." Chest **118**(2): 503-508.

Egeland, N. G., et al. (2013). "Spinal nociceptive hyperexcitability induced by experimental disc herniation is associated with enhanced local expression of Csf1 and FasL." Pain **154**(9): 1743-1748.

Eyre, D. R. and H. Muir (1977). "Quantitative analysis of types I and II collagens in human intervertebral discs at various ages." Biochim Biophys Acta **492**(1): 29-42.

Fairbank, J. C. and P. B. Pynsent (2000). "The Oswestry Disability Index." Spine (Phila Pa 1976) **25**(22): 2940-2952; discussion 2952.

Fillingim, R. B. and T. J. Ness (2000). "Sex-related hormonal influences on pain and analgesic responses." Neurosci Biobehav Rev **24**(4): 485-501.

Freemont, A. J., et al. (2002). "Nerve growth factor expression and innervation of the painful intervertebral disc." J Pathol **197**(3): 286-292.

Gauriau, C. and J. F. Bernard (2002). "Pain pathways and parabrachial circuits in the rat." Exp Physiol **87**(2): 251-258.

Gjerstad, J. (2007). "Genetic susceptibility and development of chronic non-malignant back pain." Rev Neurosci **18**(1): 83-91.

Gjerstad, J., et al. (2005). "Changes in gene expression of Zif, c-fos and cyclooxygenase-2 associated with spinal long-term potentiation." Neuroreport **16**(13): 1477-1481.

Gottfried, E., et al. (2008). "Expression of CD68 in non-myeloid cell types." Scand J Immunol **67**(5): 453-463.

Grotle, M., et al. (2003). "Cross-cultural adaptation of the Norwegian versions of the Roland-Morris Disability Questionnaire and the Oswestry Disability Index." J Rehabil Med **35**(5): 241-247.

Hara, K. and R. A. Harris (2002). "The anesthetic mechanism of urethane: the effects on neurotransmitter-gated ion channels." Anesth Analg **94**(2): 313-318, table of contents.

Harigai, M., et al. (2008). "Excessive production of IFN-gamma in patients with systemic lupus erythematosus and its contribution to induction of B lymphocyte stimulator/B cell-activating factor/TNF ligand superfamily-13B." J Immunol **181**(3): 2211-2219.

Hartung, H. P., et al. (1992). "Inflammatory mediators in demyelinating disorders of the CNS and PNS." J Neuroimmunol **40**(2-3): 197-210.

Hashioka, S., et al. (2011). "STAT3 inhibitors attenuate interferon-gamma-induced neurotoxicity and inflammatory molecule production by human astrocytes." Neurobiol Dis **41**(2): 299-307.

Hjornevik, T., et al. (2010). "Spinal long-term potentiation is associated with reduced opioid neurotransmission in the rat brain." Clin Physiol Funct Imaging **30**(4): 285-293.

Hoffman, D. S., et al. (1981). "Neuronal activity in medullary dorsal horn of awake monkeys trained in a thermal discrimination task. I. Responses to innocuous and noxious thermal stimuli." J Neurophysiol **46**(3): 409-427.

Holness, C. L., et al. (1993). "Macrosialin, a mouse macrophage-restricted glycoprotein, is a member of the lamp/lgp family." J Biol Chem **268**(13): 9661-9666.

Holness, C. L. and D. L. Simmons (1993). "Molecular cloning of CD68, a human macrophage marker related to lysosomal glycoproteins." Blood **81**(6): 1607-1613.

Hu, X. and L. B. Ivashkiv (2009). "Cross-regulation of signaling pathways by interferon-gamma: implications for immune responses and autoimmune diseases." Immunity **31**(4): 539-550.

Ikeda, H., et al. (2003). "Synaptic plasticity in spinal lamina I projection neurons that mediate hyperalgesia." Science **299**(5610): 1237-1240.

Ikeda, T., et al. (1996). "Pathomechanism of spontaneous regression of the herniated lumbar disc: histologic and immunohistochemical study." J Spinal Disord **9**(2): 136-140.

Imbeaud, S., et al. (2005). "Towards standardization of RNA quality assessment using user-independent classifiers of microcapillary electrophoresis traces." Nucleic Acids Res **33**(6): e56.

Jacobsen, L. M., et al. (2010). "Catechol-O-methyltransferase (COMT) inhibition reduces spinal nociceptive activity." Neurosci Lett **473**(3): 212-215.

Jacobsen, L. M., et al. (2012). "The COMT rs4680 Met allele contributes to long-lasting low back pain, sciatica and disability after lumbar disc herniation." Eur J Pain **16**(7): 1064-1069.

Johnstone, B. and M. T. Bayliss (1995). "The large proteoglycans of the human intervertebral disc. Changes in their biosynthesis and structure with age, topography, and pathology." Spine (Phila Pa 1976) **20**(6): 674-684.

Julius, D. and A. I. Basbaum (2001). "Molecular mechanisms of nociception." Nature **413**(6852): 203-210.

Kallakuri, S., et al. (2005). "The effects of epidural application of allografted nucleus pulposus in rats on cytokine expression, limb withdrawal and nerve root discharge." Eur Spine J **14**(10): 956-964.

Kawaguchi, S., et al. (2001). "Immunophenotypic analysis of the inflammatory infiltrates in herniated intervertebral discs." Spine (Phila Pa 1976) **26**(11): 1209-1214.

Kawakami, M., et al. (1996). "Pathomechanism of pain-related behavior produced by allografts of intervertebral disc in the rat." Spine (Phila Pa 1976) **21**(18): 2101-2107.

Kerr, R. C., et al. (1998). "GluR1 and GluR2/3 subunits of the AMPA-type glutamate receptor are associated with particular types of neurone in laminae I-III of the spinal dorsal horn of the rat." Eur J Neurosci **10**(1): 324-333.

Khazen, W., et al. (2005). "Expression of macrophage-selective markers in human and rodent adipocytes." FEBS Lett **579**(25): 5631-5634.

Kim, K., et al. (2010). "Interferon-gamma gene polymorphisms associated with susceptibility to systemic lupus erythematosus." Ann Rheum Dis **69**(6): 1247-1250.

Kokubo, Y., et al. (2008). "Herniated and spondylotic intervertebral discs of the human cervical spine: histological and immunohistological findings in 500 en bloc surgical samples. Laboratory investigation." J Neurosurg Spine **9**(3): 285-295.

Kruglyak, L. and D. A. Nickerson (2001). "Variation is the spice of life." Nat Genet **27**(3): 234-236.

Kumar, A. and B. Ghosh (2008). "A single nucleotide polymorphism (A --> G) in intron 3 of IFNgamma gene is associated with asthma." Genes Immun **9**(4): 294-301.

Latremoliere, A. and C. J. Woolf (2009). "Central sensitization: a generator of pain hypersensitivity by central neural plasticity." J Pain **10**(9): 895-926.

Le Maitre, C. L., et al. (2005). "The role of interleukin-1 in the pathogenesis of human intervertebral disc degeneration." Arthritis Res Ther **7**(4): R732-745.

Li-Weber, M. and P. H. Krammer (2003). "Regulation of IL4 gene expression by T cells and therapeutic perspectives." Nat Rev Immunol **3**(7): 534-543.

Lin, Q., et al. (2002). "Effects of protein kinase a activation on the responses of primate spinothalamic tract neurons to mechanical stimuli." J Neurophysiol **88**(1): 214-221.

Maggi, C. A. and A. Meli (1986a). "Suitability of urethane anesthesia for physiopharmacological investigations in various systems. Part 1: General considerations." Experientia **42**(2): 109-114.

Maggi, C. A. and A. Meli (1986b). "Suitability of urethane anesthesia for physiopharmacological investigations in various systems. Part 2: Cardiovascular system." Experientia **42**(3): 292-297.

Mamet, J., et al. (2003). "How nerve growth factor drives physiological and inflammatory expressions of acid-sensing ion channel 3 in sensory neurons." J Biol Chem **278**(49): 48907-48913.

McGrath, P. A. (1994). "Psychological aspects of pain perception." Arch Oral Biol **39 Suppl**: 55S-62S.

Medzhitov, R. (2008). "Origin and physiological roles of inflammation." Nature **454**(7203): 428-435.

Miki, K., et al. (2002). "Changes in gene expression and neuronal phenotype in brain stem pain modulatory circuitry after inflammation." J Neurophysiol **87**(2): 750-760.

Mizuno, T., et al. (2008). "Interferon-gamma directly induces neurotoxicity through a neuron specific, calcium-permeable complex of IFN-gamma receptor and AMPA GluR1 receptor." FASEB J **22**(6): 1797-1806.

Murata, Y., et al. (2006). "Changes in pain behavior and histologic changes caused by application of tumor necrosis factor-alpha to the dorsal root ganglion in rats." Spine (Phila Pa 1976) **31**(5): 530-535.

Nakamae, T., et al. (2011). "Pharmacological inhibition of tumor necrosis factor may reduce pain behavior changes induced by experimental disc puncture in the rat: an experimental study in rats." Spine (Phila Pa 1976) **36**(4): E232-236.

Nerlich, A. G., et al. (2002). "Immunolocalization of phagocytic cells in normal and degenerated intervertebral discs." Spine (Phila Pa 1976) **27**(22): 2484-2490.

Nilsson, E., et al. (2011). "Pain behavior changes following disc puncture relate to nucleus pulposus rather than to the disc injury per se: an experimental study in rats." Open Orthop J **5**: 72-77.

Ohtori, S., et al. (2006). "Up-regulation of acid-sensing ion channel 3 in dorsal root ganglion neurons following application of nucleus pulposus on nerve root in rats." Spine (Phila Pa 1976) **31**(18): 2048-2052.

Olmarker, K. (2008). "Puncture of a lumbar intervertebral disc induces changes in spontaneous pain behavior: an experimental study in rats." Spine (Phila Pa 1976) **33**(8): 850-855.

Olmarker, K., et al. (1995). "Inflammatogenic properties of nucleus pulposus." Spine (Phila Pa 1976) **20**(6): 665-669.

Olmarker, K. and K. Larsson (1998). "Tumor necrosis factor alpha and nucleus-pulposus-induced nerve root injury." Spine (Phila Pa 1976) **23**(23): 2538-2544.

Olmarker, K., et al. (1993). "Autologous nucleus pulposus induces neurophysiologic and histologic changes in porcine cauda equina nerve roots." Spine (Phila Pa 1976) **18**(11): 1425-1432.

Olsen, M. B., et al. (2012). "Pain intensity the first year after lumbar disc herniation is associated with the A118G polymorphism in the opioid receptor mu 1 gene: evidence of a sex and genotype interaction." J Neurosci **32**(29): 9831-9834.

Pedersen, L. M. and J. Gjerstad (2008). "Spinal cord long-term potentiation is attenuated by the NMDA-2B receptor antagonist Ro 25-6981." Acta Physiol (Oxf) **192**(3): 421-427.

Pedersen, L. M., et al. (2010). "Spinal cord long-term potentiation (LTP) is associated with increased dorsal horn gene expression of IL-1beta, GDNF and iNOS." Eur J Pain **14**(3): 255-260.

Pedersen, L. M., et al. (2005). "Induction of long-term potentiation in single nociceptive dorsal horn neurons is blocked by the CaMKII inhibitor AIP." Brain Res **1041**(1): 66-71.

Popovich, P. G., et al. (1997). "Cellular inflammatory response after spinal cord injury in Sprague-Dawley and Lewis rats." J Comp Neurol **377**(3): 443-464.

Popratiloff, A., et al. (1996). "AMPA receptor subunits underlying terminals of fine-caliber primary afferent fibers." J Neurosci **16**(10): 3363-3372.

Rand, N., et al. (1997). "Murine nucleus pulposus-derived cells secrete interleukins-1-beta, -6, and -10 and granulocyte-macrophage colony-stimulating factor in cell culture." Spine (Phila Pa 1976) **22**(22): 2598-2601; discussion 2602.

Rang, H. P., et al. (1991). "Chemical activation of nociceptive peripheral neurones." Br Med Bull **47**(3): 534-548.

Renstrom, A., et al. (2001). "Working with male rodents may increase risk of allergy to laboratory animals." Allergy **56**(10): 964-970.

Rexed, B. (1952). "The cytoarchitectonic organization of the spinal cord in the cat." J Comp Neurol **96**(3): 414-495.

Risbud, M. V. and I. M. Shapiro (2014). "Role of cytokines in intervertebral disc degeneration: pain and disc content." Nat Rev Rheumatol **10**(1): 44-56.

Robertson, B., et al. (1997). "Interferon-gamma receptors in nociceptive pathways: role in neuropathic pain-related behaviour." Neuroreport **8**(5): 1311-1316.

Rosen, L. B., et al. (1994). "Membrane depolarization and calcium influx stimulate MEK and MAP kinase via activation of Ras." Neuron **12**(6): 1207-1221.

Rothwell, N. J., et al. (1996). "Cytokines and their receptors in the central nervous system: physiology, pharmacology, and pathology." Pharmacol Ther **69**(2): 85-95.

Rothwell, N. J. and P. J. Strijbos (1995). "Cytokines in neurodegeneration and repair." Int J Dev Neurosci **13**(3-4): 179-185.

Schafers, M. and L. Sorkin (2008). "Effect of cytokines on neuronal excitability." Neurosci Lett **437**(3): 188-193.

Seguin, C. A., et al. (2005). "Tumor necrosis factor-alpha modulates matrix production and catabolism in nucleus pulposus tissue." Spine (Phila Pa 1976) **30**(17): 1940-1948.

Serhan, C. N. and J. Savill (2005). "Resolution of inflammation: the beginning programs the end." Nat Immunol **6**(12): 1191-1197.

Shamji, M. F., et al. (2010). "Proinflammatory cytokine expression profile in degenerated and herniated human intervertebral disc tissues." Arthritis Rheum **62**(7): 1974-1982.

Sommer, C. (1999). "[Animal studies on neuropathic pain: the role of cytokines and cytokine receptors in pathogenesis and therapy]." Schmerz **13**(5): 315-323.

Sugiura, Y., et al. (1986). "Central projections of identified, unmyelinated (C) afferent fibers innervating mammalian skin." Science **234**(4774): 358-361.

Takebayashi, T., et al. (2001). "Effect of nucleus pulposus on the neural activity of dorsal root ganglion." Spine (Phila Pa 1976) **26**(8): 940-945.

Tanga, F. Y., et al. (2005). "The CNS role of Toll-like receptor 4 in innate neuroimmunity and painful neuropathy." Proc Natl Acad Sci U S A **102**(16): 5856-5861.

Todd, A. J. (2002). "Anatomy of primary afferents and projection neurones in the rat spinal dorsal horn with particular emphasis on substance P and the neurokinin 1 receptor." Exp Physiol **87**(2): 245-249.

Todd, A. J. (2010). "Neuronal circuitry for pain processing in the dorsal horn." Nat Rev Neurosci **11**(12): 823-836.

Tracey, I. (2008). "Imaging pain." Br J Anaesth **101**(1): 32-39.

Tsuda, M., et al. (2009). "IFN-gamma receptor signaling mediates spinal microglia activation driving neuropathic pain." Proc Natl Acad Sci U S A **106**(19): 8032-8037.

Urban, J. P. and S. Roberts (2003). "Degeneration of the intervertebral disc." Arthritis Res Ther **5**(3): 120-130.

Vikman, K. S., et al. (2003). "Interferon-gamma induces characteristics of central sensitization in spinal dorsal horn neurons in vitro." Pain **106**(3): 241-251.

Vikman, K. S., et al. (2005). "Increased responsiveness of rat dorsal horn neurons in vivo following prolonged intrathecal exposure to interferon-gamma." Neuroscience **135**(3): 969-977.

Wagner, R. and R. R. Myers (1996). "Endoneurial injection of TNF-alpha produces neuropathic pain behaviors." Neuroreport **7**(18): 2897-2901.

Watkins, L. R., et al. (2001). "Glial activation: a driving force for pathological pain." Trends Neurosci **24**(8): 450-455.

Winkelstein, B. A., et al. (2002). "The role of mechanical deformation in lumbar radiculopathy: an in vivo model." Spine (Phila Pa 1976) **27**(1): 27-33.

Woolf, C. J. (2010). "What is this thing called pain?" J Clin Invest **120**(11): 3742-3744.

Woolf, C. J. and M. W. Salter (2000). "Neuronal plasticity: increasing the gain in pain." Science **288**(5472): 1765-1769.

Xu, Q., et al. (2008). "Activation of the neuronal extracellular signal-regulated kinase 2 in the spinal cord dorsal horn is required for complete Freund's adjuvant-induced pain hypersensitivity." J Neurosci **28**(52): 14087-14096.

Yabuki, S., et al. (1998). "Acute effects of nucleus pulposus on blood flow and endoneurial fluid pressure in rat dorsal root ganglia." Spine (Phila Pa 1976) **23**(23): 2517-2523.

Zhang, X., et al. (2005). "NGF rapidly increases membrane expression of TRPV1 heat-gated ion channels." EMBO J **24**(24): 4211-4223.

Appendix I

Procedure for RNA isolation

1. The Nucleus Pulposus tissue was transferred to a pre-cooled 2.0 ml PCR clean eppendorf tube and 0.8 ml Isol-RNA Lysis Reagent (5PRIME) was added.
2. 3 sterile metal balls were added to each sample, and the tissue was homogenized by aid of a mixer mill (frequency: 30, time: 4 x 30 seconds).
3. The sample was incubated for 5 min at room temperature.
4. The sample was centrifuged at 12 000 g for 5 min at 4 °C. The supernatant was transferred to a new eppendorf tube.
5. 0.2 ml chloroform was added. The sample was shaken vigorously by hand for 15 sec and incubated for 3 min at room temperature.
6. The sample was centrifuged at 12 000 g for 15 min at 4 °C.
7. The water phase was transferred to a new Eppendorf tube. 0.5 ml isopropanol was added. The content was mixed well and incubated for 10 min at room temperature.
8. The sample was centrifuged at 12 000 g for 15 min at 4 °C.
9. The supernatant was removed and the RNA pellet was washed with 1 ml 75 % EtOH, mixed and vortexed.
10. The sample was centrifuged at 12 000 g for 5 min at 4 °C.
11. The supernatant was removed. The pellet was dried for 15-30 min at room temperature, dissolved in 10 µl RNase free water and kept on ice.
12. The sample was incubated for 10 min at 65 °C, placed on ice, spun, placed back on ice and mixed by a pipette.
13. The sample was then frozen and stored at -80 °C.
14. 1 µl of RNA was used to measure the concentration with a NanoDrop 8000 Spectrophotometer (Thermo Scientific).

Appendix II

Procedure for evaluation of RNA quality by on-chip electrophoresis using "Agilent RNA 6000 Nano Kit" (Agilent Technologies, Waldbronn, Germany)

The reagents were equilibrated to room temperature for 30 minutes before use.

1. 550 µl of the RNA 6000 Nano gel matrix was transferred to a spin filter and centrifuged at 1500 g for 10 min at room temperature. An aliquot of 65 µl of the filtered gel was transferred to a 0.5 ml microfuge tube.
2. The RNA 6000 Nano dye concentrate was vortexed for 10 sec and spun down. 1 µl of the dye was added to the filtered gel. The solution was vortexed well and centrifuged at 13 000 g for 10 min at room temperature.
3. The RNA samples were diluted to a final concentration of 300 ng/µl and heat denatured at 70 °C for 2 min.
4. 350 µl of RNase Away was loaded to a microchip and run for 1 min on the Bioanalyzer for decontamination of the electrodes. The procedure was repeated with 350 µl RNase-free water for 10 sec.
5. 9 µl of the gel-dye mix was loaded to the well marked ^G on a new RNA 6000 Nano microchip.
6. The microchip was mounted on the chip priming station. The priming station was closed and pressure was applied to the microchip for 30 sec by a plunger.
7. 9 µl of the gel-dye mix wasloaded to the wells marked G.
8. 5 µl of the RNA 6000 Nano marker was loaded to all 12 test-wells and to the ladder-well.
9. The standard ladder was heat denatured at 70 °C for 2 min. 1 µl of the ladder was loaded to the well marked with the ladder.
10. 1 µl of the samples were loaded to the test-wells.
11. The microchip was vortexed at 2000 rpm for 1 min, and then run on the Bioanalyzer.
12. After the Bioanalyzer had completed the analysis-program, 350 µl of RNase-free water was loaded to a microchip and run for 10 sec on the Bioanalyzer for decontamination of the electrodes.

Appendix III

Procedure for cDNA synthesis using "First Strand cDNA Synthesis Kit for RT-PCR (AMV)" (Roche Diagnostics, Mannheim, Germany)

All reagents and samples were kept on ice unless specified otherwise.

1. 1.5 µg of RNA was mixed with water to a total volume of 4.5 µl in 0.5 ml Eppendorf tubes.
2. Mixture 1 was prepared:

Reagent:	volume/sample
Random Primer p(dN)	1.5 µl
Deoxynucleotide Mix	1.5 µl
Total	3.0 µl

3. 3 µl of mixture 1 was added to each sample. The tubes were vortexed and spun down.
4. The tubes were incubated at 65 °C for 15 min, and then put directly on ice.
5. Mixture 2 was prepared:

Reagent	volume/sample
10 x Reaction Buffer	1.50 µl
25 mM $MgCl_2$	3.00 µl
RNase Inhibitor 50 U/ µl	0.68 µl
AMV Reverse Transcriptase	0.53 µl
Sterile water	1.80 µl
Total	7.51 µl

6. 7.5 µl of mixture 2 was added to each tube. The tubes were vortexed and spun down.
7. The reverse transcription reaction was run on the PCR machine at the following program: 42 °C for 60 min, 99 °C for 5 min and 4 °C for 5 min.
8. Each sample was added 135 µl of TE-buffer to a final concentration of 10 ng/µl, mixed and spun down.
9. The samples were stored at – 80 °C.

Appendix IV

Layout for the 96-well PCR array.

	1	2	3	4	5	6	7	8	9	10	11	12
A	Adipoq	Aimp1	Areg	Bmp1	Bmp2	Bmp3	Bmp4	Bmp5	Bmp6	Bmp7	C5	Cd40lg
B	Cd70	Cntf	Csf1	Csf2	Csf3	Ctf1	Faslg	Fgf10	Gdf15	Gdf5	Gdf9	Grem1
C	Ifna1	Ifna2	Ifna4	Ifnb1	Ifng	Il10	Il11	Il12a	Il12b	Il13	Il15	Il16
D	Il17a	Il17b	Il17f	Il18	Il1a	Il1b	Il1rn	Il2	Il20	Il21	Il22	Il23a
E	Il24	Il27	Il3	Il33	Il4	Il5	Il6	Il7	Il9	Inha	Inhba	Lif
F	Lta	Ltb	Mif	Mstn	Nampt	Nodal	Nrg1	Osm	Scgb3a1	Spp1	Tgfb1	Tgfb2
G	Thpo	Tnf	Tnfrsf11b	Tnfsf10	Tnfsf11	Tnfsf12	Tnfsf13	Tnfsf15	Tnfsf18	Tnfsf4	Tnfsf9	Vegfa
H	Actb	B2m	Hprt1	Ldha	Rplp1	RGDC	RTC	RTC	RTC	PPC	PPC	PPC

Gene table: RT^2 Profiler PCR array.

Position	Unigene	GeneBank	Symbol	Description
A01	Rn.24299	NM_144744	Adipoq	Adiponectin, C1Q and collagen domain containing
A02	Rn.3192	NM_053757	Aimp1	Aminoacyl tRNA synthetase complex-interacting multifunctional protein 1
A03	Rn.10568	NM_017123	Areg	Amphiregulin
A04	Rn.9305	NM_031323	Bmp1	Bone morphogenetic protein 1
A05	Rn.90931	NM_017178	Bmp2	Bone morphogenetic protein 2
A06	Rn.208979	NM_017105	Bmp3	Bone morphogenetic protein 3
A07	Rn.10318	NM_012827	Bmp4	Bone morphogenetic protein 4
A08	Rn.135799	NM_001108168	Bmp5	Bone morphogenetic protein 5
A09	Rn.40476	NM_013107	Bmp6	Bone morphogenetic protein 6
A10	Rn.18030	XM_342591	Bmp7	Bone morphogenetic protein 7
A11	Rn.21259	XM_342421	C5	Complement component 5
A12	Rn.44218	NM_053353	Cd40lg	CD40 ligand
B01	Rn.103013	NM_001106878	Cd70	Cd70 molecule
B02	Rn.6067	NM_013166	Cntf	Ciliary neurotrophic factor
B03	Rn.83632	NM_023981	Csf1	Colony stimulating factor 1 (macrophage)
B04	Rn.44285	XM_340799	Csf2	Colony stimulating factor 2 (granulocyte-macrophage)
B05	Rn.53973	NM_017104	Csf3	Colony stimulating factor 3 (granulocyte)
B06	Rn.10253	NM_017129	Ctf1	Cardiotrophin 1
B07	Rn.9725	NM_012908	Faslg	Fas ligand (TNF superfamily, member 6)
B08	Rn.44439	NM_012951	Fgf10	Fibroblast growth factor 10
B09	Rn.44228	NM_019216	Gdf15	Growth differentiation factor 15
B10	Rn.127822	XM_001066344	Gdf5	Growth differentiation factor 5
B11	Rn.42874	NM_021672	Gdf9	Growth differentiation factor 9
B12	Rn.42929	NM_019282	Grem1	Gremlin 1, cysteine knot superfamily, homolog (Xenopus laevis)
C01	Rn.196548	NM_001014786	Ifna1	Interferon-alpha 1
C02	N/A	XM_233152	Ifna2	Interferon alpha family, gene 2
C03	Rn.218577	NM_001106667	Ifna4	Interferon, alpha 4
C04	Rn.138105	NM_019127	Ifnb1	Interferon beta 1, fibroblast
C05	Rn.10795	NM_138880	Ifng	Interferon gamma
C06	Rn.9868	NM_012854	Il10	Interleukin 10
C07	Rn.198483	NM_133519	Il11	Interleukin 11

C08	Rn.207199	NM_053390	Il12a	Interleukin 12a
C09	Rn.48686	NM_022611	Il12b	Interleukin 12b
C10	Rn.9921	NM_053828	Il13	Interleukin 13
C11	Rn.2490	NM_013129	Il15	Interleukin 15
C12	Rn.104665	NM_001105749	Il16	Interleukin 16
D01	Rn.218513	NM_001106897	Il17a	Interleukin 17A
D02	Rn.50003	NM_053789	Il17b	Interleukin 17B
D03	Rn.34022	NM_001015011	Il17f	Interleukin 17F
D04	Rn.11118	NM_019165	Il18	Interleukin 18
D05	Rn.12300	NM_017019	Il1a	Interleukin 1 alpha
D06	Rn.9869	NM_031512	Il1b	Interleukin 1 beta
D07	Rn.162640	NM_022194	Il1rn	Interleukin 1 receptor antagonist
D08	Rn.9871	NM_053836	Il2	Interleukin 2
D09	Rn.222008	NM_001143881	Il20	Interleukin 20
D10	Rn.214949	NM_001108943	Il21	Interleukin 21
D11	Rn.195879	XM_576228	Il22	Interleukin 22
D12	Rn.81073	NM_130410	Il23a	Interleukin 23, alpha subunit p19
E01	Rn.48710	NM_133311	Il24	Interleukin 24
E02	N/A	XM_344962	Il27	Interleukin 27
E03	Rn.10652	NM_031513	Il3	Interleukin 3
E04	Rn.106849	NM_001014166	Il33	Interleukin 33
E05	Rn.108255	NM_201270	Il4	Interleukin 4
E06	Rn.44227	NM_021834	Il5	Interleukin 5
E07	Rn.9873	NM_012589	Il6	Interleukin 6
E08	Rn.10793	NM_013110	Il7	Interleukin 7
E09	Rn.92374	NM_001105747	Il9	Interleukin 9
E10	Rn.8831	NM_012590	Inha	Inhibin alpha
E11	Rn.9874	NM_017128	Inhba	Inhibin beta-A
E12	Rn.44379	NM_022196	Lif	Leukemia inhibitory factor
F01	Rn.160577	NM_080769	Lta	Lymphotoxin alpha (TNF superfamily, member 1)
F02	Rn.203016	NM_212507	Ltb	Lymphotoxin beta (TNF superfamily, member 3)
F03	Rn.2661	NM_031051	Mif	Macrophage migration inhibitory factor
F04	Rn.44460	NM_019151	Mstn	Myostatin
F05	Rn.203508	NM_177928	Nampt	Nicotinamide phosphoribosyltransferase
F06	Rn.218528	NM_001106394	Nodal	Nodal homolog (mouse)
F07	Rn.37438	NM_031588	Nrg1	Neuregulin 1
F08	Rn.127158	NM_001006961	Osm	Oncostatin M
F09	Rn.30648	NM_001013180	Scgb3a1	Secretoglobin, family 3A, member 1
F10	Rn.8871	NM_012881	Spp1	Secreted phosphoprotein 1
F11	Rn.40136	NM_021578	Tgfb1	Transforming growth factor, beta 1
F12	Rn.24539	NM_031131	Tgfb2	Transforming growth factor, beta 2
G01	Rn.10576	NM_031133	Thpo	Thrombopoietin
G02	Rn.2275	NM_012675	Tnf	Tumor necrosis factor (TNF superfamily, member 2)
G03	Rn.202973	NM_012870	Tnfrsf11b	Tumor necrosis factor receptor superfamily, member 11b
G04	Rn.83627	NM_145681	Tnfsf10	Tumor necrosis factor (ligand) superfamily, member 10
G05	Rn.64517	NM_057149	Tnfsf11	Tumor necrosis factor (ligand) superfamily, member 11
G06	Rn.3211	NM_001001513	Tnfsf12	Tumor necrosis factor ligand superfamily member 12
G07	Rn.19955	NM_001009623	Tnfsf13	Tumor necrosis factor (ligand) superfamily, member 13
G08	Rn.84873	NM_145765	Tnfsf15	Tumor necrosis factor (ligand) superfamily, member 15
G09	N/A	XM_344166	Tnfsf18	Tumor necrosis factor (ligand) superfamily, member 18
G10	Rn.30043	NM_053552	Tnfsf4	Tumor necrosis factor (ligand) superfamily, member 4
G11	Rn.185237	NM_181384	Tnfsf9	Tumor necrosis factor (ligand) superfamily, member 9
G12	Rn.1923	NM_031836	Vegfa	Vascular endothelial growth factor A
H01	Rn.94978	NM_031144	Actb	Actin, beta
H02	Rn.1868	NM_012512	B2m	Beta-2 microglobulin
H03	Rn.47	NM_012583	Hprt1	Hypoxanthine phosphoribosyltransferase 1
H04	Rn.107896	NM_017025	Ldha	Lactate dehydrogenase A
H05	Rn.973	NM_001007604	Rplp1	Ribosomal protein, large, P1
H06	N/A	U26919	RGDC	Rat Genomic DNA Contamination
H07	N/A	SA_00104	RTC	Reverse Transcription Control
H08	N/A	SA_00104	RTC	Reverse Transcription Control
H09	N/A	SA_00104	RTC	Reverse Transcription Control
H10	N/A	SA_00103	PPC	Positive PCR Control
H11	N/A	SA_00103	PPC	Positive PCR Control
H12	N/A	SA_00103	PPC	Positive PCR Control

Procedure for Real time PCR for RT Profiler PCR array (Qiagen, Cat.no. 330231 PARN-021ZA)

All reagents and samples were kept on ice unless specified otherwise.

1. Pooled cDNA samples from the exposed NP group and native NP group were constructed.

2. A master mix was prepared:

Reagent	volume/sample
ddH_2O	1248 µl
2X RT SYBR Green Mastermix	1350 µl
cDNA (10ng/µl) from pooled NP exposed or native	102 µl
Total	2700 µl

3. 25 µl master mix was loaded to each well on the 96 PCR plate, already containing the respective primers.

4. The PCR plate was sealed with a plastic film and spun down at 2500 rpm.

5. The qPCR reaction was run at the following schedule: 95°C for 10 minutes, followed by 40 cycles of 95°C for 15 seconds and 60 °C for 60 seconds.

Appendix V

Procedure for qPCR

All reagents and samples were kept on ice unless specified otherwise.

6. A master mix was prepared:

Reagent	volume/sample
ddH_2O	5.22 µl
Perfecta SYBR Green FastMix	10.0 µl
Primer forward (25 pmol/ µl)	0.21 µl
Primer reverse (25 pmol/ µl)	0.21 µl
Total	15.64 µl

7. The cDNA samples used for β-actin analysis were diluted: 1 µl cDNA (10 ng/µl) + 9 µl RNase free water.
8. 8 µl from three different cDNA samples (10 ng/µl) were mixed to give a stock cDNA solution. A dilution series used to generate a standard curve for each was prepared.

Dilution series nr	cDNA	RNase free water	
1	4.35 µl	undiluted	100ng
2	6 µl	+ 18µl	25ng
3	6 µl from nr 2	+ 18 µl	6.25ng
4	6 µl from nr 3	+ 18 µl	1.56ng
5	6 µl from nr 4	+ 18 µl	0.39ng
6	6 µl from nr 5	+ 18 µl	0.0975ng

9. 15.65 µl master mix was loaded to each well on a 96 well plate.
10. 4.35 µl ddH_2O was added to the non-template control (NTC) wells.
11. 4.35 µl sample cDNA or pre-diluted samples for β-actin analysis or dilution series samples were transferred to the PCR-plate in two parallels and mixed well.
12. The PCR plate was sealed with a plastic film and spun down at 2500 rpm.
13. The qPCR reaction was run at the following schedule: 90 °C for 2 min followed by 40 cycles of 95 °C for 10 sec and finally 60 °C for 30 sec.

Appendix VI

Procedure for DNA isolating using FlexiGene DNA kit (Qiagene, Hilsen, Germany)

1. Transfer the sample to an 50 ml centrifuge tube and homogenize the sample using a rotor-stator homogenizer for at least 30 s at maximum speed.
2. Add 25 ml Buffer FG1 and mix by inverting the tube 5 times.
3. Centrifuge for 5 min at 2000 x g in a swing-out rotor.
4. Discard supernatant and leave the tube inverted on absorbent paper for 2 min. Make sure that the pellet remain in the tube.
5. Add 5 ml Buffer FG2 and 50 µl Qiagen protease. Vortex immediately until the pellet is completely homogenized.
6. Invert the tube 3 times and incubate at 65 °C for at least 25 min.
7. Vortex for 5 s and check that homogenization is complete.
8. Add 5 ml isopropanol and mix by inversion until the DNA precipitate becomes visible as threads or a clump.
9. Centrifuge for 3 min at 2000 x g.
10. Discard the supernatant briefly invert the tube on absorbent paper. Make sure that the pellet remains in the tube.
11. Add 5 ml 70 % ethanol and vortex for 5 s.
12. Centrifuge for 3 min at 2000 x g.
13. Discard the supernatant and leave the tube inverted on absorbent paper for at least 5 min. Make sure that the pellet remain in the tube.
14. Air-dry the DNA pellet until all the liquid has evaporated (at least 5 min)
15. Add 1 ml Buffer FG3, vortex for 5 s at low speed and dissolve the DNA by incubating for 1 h at 65 °C.

Appendix VII

Protocol for TaqMan SNP genotyping (Applied biosystems, USA)

All reagents and samples were kept cold unless specified otherwise.

1. 96 well plates with template DNA was spun down at 3000rpm.

2. A master mix was prepared:

Reagent	volume/sample
ddH_2O	3.46 µl
TaqMan genotyping Mastermix	1.50 µl
Probe/Primer mix	0.10 µl
Total	5.06 µl

3. 5 µl of master mix was loaded to each well on a 384 well plate.

4. 0.5 µl of template DNA (20ng/µl) was added to each well

5. 0.5 µl ddH_2O was added to the non-template control (NTC) wells

6. The PCR plate was sealed with a plastic film and spun down at 3000 rpm.

7. The PCR reaction was run at the following schedule: 50°C for 2 min and 95°C for 10 min followed by 40 cycles of 95°C for 15 sec and 60°C for 1 min.

8. The PCR plate was spun down at 3000rpm

9. Allelic discrimination was performed on the PCR machine immediately after for determination of genotypes.